Thermodynamic Modeling of the

Na_2O –, CaO –, MgO – As_2O_5 Binary Systems

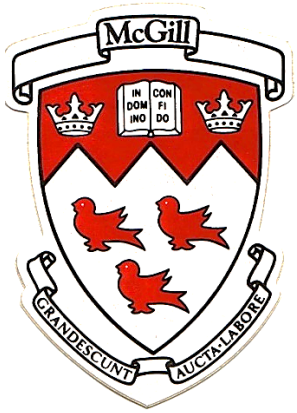

Master's Degree
Department of Mining and Materials Engineering
McGill University
Montreal, Quebec, Canada

A thesis submitted to McGill University for the fulfillment of the requirements of the Master's degree in Materials Engineering

By: Jun-Hyung Lee
Submitted August, 2019

Abstract

Arsenic is a highly toxic element found associated with certain minerals and in the drinking water in some parts of the world. Not only is arsenic dangerous, but handling it is difficult due to its volatility and tendency to absorb water. The copper industry accesses more and more arsenic containing mineral deposits due to the depletion of copper ores. Even in the gold industry, ore bodies containing significant levels of arsenic are under consideration. In pyrometallurgical and hydrometallurgical processes of such minerals, arsenic becomes a major environmental issue to be resolved for sustainable processing. One possible industrial route to minimize the environmental arsenic problem is the stabilization of arsenic oxide into a glass phase. In order to understand the fundamentals of such a stabilization process and to design the proper glass composition and operating conditions, the thermodynamic knowledge of arsenic oxides in multicomponent oxide systems is indispensable.

As part of a larger thermodynamic database for the understanding of thermodynamic behavior of arsenic oxide (arsenate, As_2O_5) in solid and liquid state, thermodynamic modeling of binary Na_2O-As_2O_5, CaO-As_2O_5 and MgO-As_2O_5 systems were performed in the present study. The Gibbs energies of all available phases in each binary system were determined based on the critical evaluation and optimization of existing thermodynamic and phase diagram data. As thermodynamic data of solid compounds and liquid solution available in literature were insufficient, the general trends in each binary arsenate systems were evaluated and used for the estimation of unknown thermodynamic properties in the course of the present thermodynamic optimization process. The Gibbs energy of the liquid solution of each binary arsenate system was described using the Modified Quasichemical Model to capture the effects short-range ordering.

All thermodynamic calculations in this study were made using the FactSage thermodynamic software.

Résumé

L'arsenic est un élément hautement toxique associé à certains minéraux et à l'eau de boisson dans certaines parties du monde. Pas seulement l'arsenic est dangereux, mais sa manipulation est difficile en raison de sa volatilité et de sa tendance à absorber l'eau. L'industrie du cuivre accède de plus en plus à des gisements minéraux contenant de l'arsenic en raison de l'épuisement des minerais de cuivre. Même dans l'industrie aurifère, des gisements contenant des niveaux importants d'arsenic sont à l'étude. Dans les procédés pyrométallurgiques et hydrométallurgiques de ces minéraux, l'arsenic devient un problème environnemental majeur à résoudre pour un traitement durable. Une voie industrielle possible pour minimiser le problème environnemental de l'arsenic est la stabilisation de l'oxyde d'arsenic en une phase de verre. Afin de comprendre les principes fondamentaux d'un tel processus de stabilisation et de concevoir la composition de verre appropriée et les conditions de fonctionnement, la connaissance thermodynamique des oxydes d'arsenic dans les systèmes d'oxyde à plusieurs composants est indispensable.

Dans le cadre d'une base de données thermodynamiques plus large pour la compréhension du comportement thermodynamique de l'oxyde d'arsenic (arséniate, As2O5) à l'état solide et liquide, la modélisation thermodynamique des systèmes binaires Na2O-As2O5, CaO-As2O5 et MgO-As2O5 a été réalisée dans la présente étude. Les énergies de Gibbs de toutes les phases disponibles dans chaque système binaire ont été déterminées sur la base de l'évaluation critique et de l'optimisation des données thermodynamiques et de diagramme de phases existantes. Les données thermodynamiques des composés solides et des solutions liquides disponibles dans la littérature étant insuffisantes, les tendances générales de chaque système d'arséniate binaire ont été évaluées et utilisées pour l'estimation de propriétés thermodynamiques inconnues au cours du présent processus d'optimisation thermodynamique. L'énergie de Gibbs de la solution liquide de chaque

système d'arséniate binaire a été décrite à l'aide du modèle quasi-chimique modifié pour capturer l'ordre des effets à court terme. Tous les calculs thermodynamiques de cette étude ont été effectués à l'aide du logiciel thermodynamique FactSage.

Acknowledgement

I sincerely thank Prof. In-Ho Jung for allowing me the opportunity to work on this project and all his kind support and patience over the course of this work.

I am especially indebted to Sunyong Kwon, who without this project may not have been possible, for his tireless guidance throughout the work, teachings too numerous to count and providing support for my (many) shortcomings.

I would like to thank all the members of the High-Temperature Thermochemistry Laboratory for providing an enjoyable and encouraging work environment, especially Dr. Pierre Hudon for all the valuable information and lessons imparted, Dr. Dong-Geun Kim for his help, and Kota Matsuo for the frequent yet riveting discussions.

I am very thankful and appreciative to the administrative staff of the Mining and Materials Engineering Department for their efforts in helping to ensure I may work without worry. In particular, the efforts of Ms. Barbara Hanley for always being helpful and patient.

Finally, I would like to thank my family for their unconditional support throughout my life, for which nothing is impossible with their love and support.

Table of Contents

Table of Tables

Table of Figures

1. Introduction

Arsenic is a highly toxic element which often contaminates drinking water. Long-term exposure to inorganic arsenic through drinking contaminated water can lead to skin lesions and skin cancer [1]. Concentrated inorganic arsenic can be produced by industrial processes such as mining and smelting of cobalt and gold as byproducts.

Yellowknife, Northwest Territories, Canada is the location of Giant Mine, one of the greatest environmental issues faced in Canada. Presently shut down, it was where a large amount of gold was mined from, operating from the 1930s till early 2000, producing roughly 220 tons of pure gold. Found associated with the gold, however, was an even greater amount of arsenic: over 237 000 tons in the form of arsenic oxide. The arsenic tailings produced after the gold was processed were simply left in chambers and stopes located at the mine site. The arsenic did not spread out far from the site, so the contamination remains under control as the cold weather helps keep the arsenic frozen. Coolant pipes were placed throughout the area to help keep the arsenic frozen, however, this only proved to be a temporary solution as it requires constant investment in order to maintain it. Furthermore, with the onset of global warming, the area is beginning to thaw, and the coolant pipes are proving to be less and less effective over time. As such, the Canadian government has launched an initiative in order to rectify this problem [2].

As a first step to the arsenic removal or stabilization, it is important to know the thermodynamic properties of arsenic containing phases which can be used to sequester arsenic by finding solid and liquid phases with a low activity of arsenic. Accurate thermodynamic database developed via the Calculation of Phase Diagram (CALPHAD) method can become a useful research tool for this purpose because the complex chemical reaction and phase equilibria of arsenic containing species

can be calculated at any temperature and composition once the good thermodynamic database containing arsenic species is available. The purpose of the present study is the development of accurate thermodynamic database for binary arsenate (As_2O_5) systems.

2. Methodology

2.1 CALPHAD Methodology

In the CALPHAD method, the Gibbs energy of each phase is parameterized as a function of temperature, pressure and compositions. First, to develop a self-consistent database, these parameters are assessed by reproducing the thermodynamic property data which are empirically measured and considered reliable. Afterwards, these Gibbs energies are used to calculate the phase diagram and compared with the experimental data. Finally, the Gibbs energies are adjusted so that the thermodynamic property and phase diagram data are reproduced simultaneously. This process of determining parameters is called 'thermodynamic optimization'.

The reliability of collected literature data must be assessed before applying them towards thermodynamic optimizations. It may be frequently seen that the experimental data and results differ from one investigation to another, whether it may be a slight discrepancy in reported values or conclusions that directly contradict one another. Some of these inconsistencies can be resolved by critically evaluating the experimental data based on sample preparation, experimental procedures and characterization. Great scrutiny must be placed upon possible sources of experimental error. Even with this mindfulness, the accuracy of some experimental investigations may be difficult to evaluate on occasion, typically due to a lacking explanation as to the details of the work. This may be rectified during the process of thermodynamic optimization. For instance, the restrictions given by phase diagram data can be used to evaluate the thermodynamic properties of the relevant phases, as the two sets of data are intertwined with thermodynamic principles.

If experimental data available in literature is insufficient to perform thermodynamic optimization of a system, experiments should be conducted. This is often the case for systems involving As_2O_5,

due to the volatility and hygroscopic nature of As_2O_5. Some attempts were made to conduct phase diagram experiments in this study, however, due to the experimental challenges associated with arsenic containing systems, the results were excluded in the following optimizations. An outline of the experimental work and challenges faced may be seen in Appendix B.

2.1.1 Gibbs Energy of Pure Compounds

The Gibbs energy of pure compound at constant pressure is expressed as shown below:

$$G_T^o = H_T^o - TS_T^o \quad \textbf{(1)}$$

$$H_T^o = \Delta H_{298K}^o + \int_{298\ K}^{T} C_P\ dT \quad \textbf{(2)}$$

$$S_T^o = S_{298K}^o + \int_{298\ K}^{T} \frac{C_P}{T}\ dT \quad \textbf{(3)}$$

where G_T^o, H_T^o, and S_T^o are the standard Gibbs energy, enthalpy and entropy respectively, at temperature T, for a given stoichiometric compound. ΔH_{298}^o is the standard enthalpy of formation of the compound from pure elements at 298 K. S_{298}^o is the standard entropy at 298 K. C_P is the molar heat capacity which is expressed as a function of temperature according to Berman and Brown [3]. ΔH_{298}^o, S_{298}^o, and C_P are the model parameters which need to be assessed through the thermodynamic optimization process or, if possible, based on experimental data.

2.1.2 Gibbs Energy of Liquid Solutions

To have accurate thermodynamic descriptions for solution phases, it is important to choose a proper solution model which considers physical properties of the solution such as structure or short-range ordering. The well-described configuration entropy in this proper solution model will contribute to reduce the number of model parameters, thus having high predictability for multicomponent systems without introducing additional model parameters. In oxide melt, short-range ordering is known to have a prominent effect [4]. Therefore, the liquid phase of this study was described with the Modified Quasichemical Model (MQM) [5], which takes into account the short-range ordering of a solution by pair distribution. The complete description for the MQM can be found in [3-6]. A short description for the MQM is given below

In MQM, elemental component (atoms or molecules) are assumed to be distributed over the sites of a quasilattice. A binary system as an example with A and B as constituents, the following pair exchange reaction can be considered:

$$(A-A)+(B-B)=2(A-B);\Delta g_{AB} \qquad \textbf{(4)}$$

where $(i-j)$ represents a first nearest neighbor (FNN) pair, and Δg_{AB} is the reaction Gibbs energy of the pair exchange reaction, which determines the distribution of pairs. For instance, if $\Delta g_{AB} < -\infty$, $(A-B)$ will be the most stable and dominant pairs; whereas if $\Delta g_{AB} = \infty$, the number of $(A-B)$ will be close to zero. This pair exchange reaction Gibbs energy, Δg_{AB} is the model parameter to be optimized for the MQM. It should be noted that the pair exchange reaction **(4)**occurs among the second nearest neighbor (SNN) pairs in oxide melts as the interaction between cation and anion are assumed to be infinity (the reaction Gibbs energy of the FNN pairs is $-\infty$; that is, there is always O^{2-} in between cations).

The number of pairs, n_{ij}, in the MQM are defined as follows:

$$Z_A n_A = 2n_{AA} + n_{AB} \quad \textbf{(5)}$$

$$Z_B n_B = 2n_{BB} + n_{AB} \quad \textbf{(6)}$$

where n_i represents the number of moles. Z_i is the coordination number of component i, which is a model parameter to be determined based on the composition of the maximum short-range ordering in the melt.

The solution Gibbs energy of this binary system is expressed as:

$$G = n_A g_A^o + n_B g_B^o - T\Delta S^{config} + \frac{n_{AB}\Delta g_{AB}}{2} \quad \textbf{(7)}$$

where $g_i^o$is the molar Gibbs energy of the pure component i, and ΔS^{config} is the configurational entropy defined as:

$$\Delta S^{config} = -R(n_A lnX_A + n_B lnX_B + n_{AA} \ln\left(\frac{X_{AA}}{Y_A^2}\right) + n_{BB} \ln\left(\frac{X_{BB}}{Y_B^2}\right) + n_{AB} \ln\left(\frac{X_{AB}}{2Y_A Y_B}\right)) \quad \textbf{(8)}$$

where $X_i, Y_i, and\ X_{ij}$ represent mole fraction, equivalent fraction and pair fraction, respectively. Each of these fractions are defined as:

$$X_A = 1 - X_B = \frac{n_A}{n_A + n_B} \quad \textbf{(9)}$$

$$Y_A = 1 - Y_B = \frac{Z_A n_A}{Z_A n_A + Z_B n_B} = X_{AA} + \frac{X_{AB}}{2} \quad \textbf{(10)}$$

$$X_{ij} = \frac{n_{ij}}{n_{AA} + n_{BB} + n_{AB}} \quad \textbf{(11)}$$

Once the model parameter, Δg_{AB} is defined, the equilibrium pair distribution is calculated through the following equation:

$$\left(\frac{\partial G}{\partial n_{AB}}\right)_{n_A, n_B} = 0 \quad \textbf{(12)}$$

The number of pairs, n_{ij} determined by the equation **(12)**, then, are used to calculate the solution Gibbs energy defined in the equation **(7)**.

To describe configuration dependent interactions between components, the model parameter, Δg_{AB} is expanded in terms of pair fraction:

$$\Delta g_{AB} = \Delta g^{o}_{AB} + \sum_{i\geq 1} g^{i0}_{AB} X^{i}_{AA} + \sum_{j\geq 1} g^{0j}_{AB} X^{j}_{BB} \qquad \textbf{(13)}$$

where $\Delta g^{o}_{AB}, g^{i0}_{AB}$, and g^{0j}_{AB} are the model parameters which can be a function of temperature. The exponents *i* and *j* are model parameters that act as weighting factors.

2.2 Objective

The objective of this study is to develop a thermodynamic database that, through the use of the thermochemical software FactSage 7.2, may be used to help design a process in which arsenic may be sequestered as a method to reduce or eliminate arsenic pollution. In particular, thermodynamic understanding of arsenic in the form of arsenic oxide, As_2O_5 (as it is the most stable oxide form [9]), and of arsenic oxide containing systems will help to facilitate the production of stable arsenic oxide containing compounds. This understanding will provide invaluable information to not only design but optimize the process by determining what the thermodynamically maximum amount of arsenic may be contained while maintaining a sufficiently minimal chemical potential to avoid leaching. As the oxide form is of interest, a multi-component glass as a means of sequestering the arsenic is desirable. Once contained in a glass, it may be safely stored or transported without worry.

2.3 Scope of Research

In addition to As_2O_5 itself, three binary systems were investigated: Na_2O – As_2O_5, CaO – As_2O_5 and MgO – As_2O_5. Thermodynamic data are available for Na_2O, CaO and MgO in the most up to date FactSage database. While thermodynamic data for As_2O_5 are available in the FactPS database, As_2O_5 itself is not extensively utilized, as such, its thermodynamic properties were reviewed to determine the quality of the data. These three binary systems were investigated because, in addition to SiO_2, they are amongst the most commonly used components in commercial glasses. Furthermore, their properties because network modifiers is important as controlling the viscosity and glass transition temperature of the melt during processing will prove to be valuable when working to manage the volatile nature of arsenic oxide. The SiO_2 – As_2O_5 system was not investigated in this work because there was no information available about this binary system, however, this presents itself as a major barrier towards the overall objective as there are no substitutes for SiO_2 when producing a glass.

3. Thermodynamic Assessment of Pure As_2O_5

Prior to the evaluation and optimization of As_2O_5-containing binary systems, the component As_2O_5 itself must first be evaluated. The thermodynamic properties of solid As_2O_5 may be found in FactPS general compound database in FactSage. Both enthalpy of formation and standard entropy are available from the NBS Technical Note [11], a reliable source known for having good standards and data processing procedures. The heat capacity function was estimated by Pankratz [11] from 300 K to 700K. Specifics are not given as to how the estimation was made, however, provided are a number of examples to demonstrate various methods the author had used to process and calculate data. In the present work, heat capacity was re-evaluated to include the experimental work of Anderson [12], who had measured low-temperature heat capacity data using adiabatic calorimetry, as seen in Figure 3.1. The function essentially did not change from 298 K and onwards and the inclusion of low-temperature heat capacity data was to smooth the function, keeping it consistent from low-temperature to high-temperature. The upper limit of the heat capacity was adjusted to the melting temperature of As_2O_5 to be consistent with phase diagram data [11-17]. The melting temperature was reported to be a wide array of values, but at present, all phase diagram data (including systems not studied here) consistently report the same melting temperature of 740 ^oC (1013 K) and was taken as such.

The FactPS database contained no information about liquid As_2O_5, however, in order to optimize the binary and higher-order As_2O_5-containing systems, the thermodynamic properties of liquid As_2O_5 are necessary. To resolve this, the entropy of fusion of As_2O_5 was assumed to be the same as the entropy of fusion of P_2O_5. This is because they are assumed to have a periodic trend. This may be seen in similar physical behavior occurring with the two compounds, such as volatility and hygroscopicity, and reports that the two compounds share similar structural arrangements [20].

Taking this and the melting temperature of As_2O_5, the enthalpy of fusion was calculated, thus giving us thermodynamic properties for liquid As_2O_5. A summary of the thermodynamic properties of As_2O_5 can be seen in Table 3.1.

4. Critical Evaluation and Thermodynamic Optimization of the Na_2O – As_2O_5 System

4.1 Literature Review

4.1.1 Phase Diagram Data

Six stable compounds were reported to exist in the Na_2O – As_2O_5 binary system: $NaAsO_3$ (NA), $Na_4As_2O_7$ (N_2A), Na_3AsO_4 (N_3A), $Na_5As_3O_{10}$ (N_5A_3), $Na_2As_4O_{11}$ (NA_2) and $NaAs_3O_8$ (NA_3).

The melting temperatures of $NaAsO_3$, $Na_4As_2O_7$ and Na_3AsO_4 were studied by several authors who reported them to melt congruently [19-21]. The melting temperature of $Na_4As_2O_7$ was further investigated in a later work [24] as was Na_3AsO_4 [25]. $Na_5As_3O_{10}$ was reported to melt incongruently [19,20]. The remaining compounds, $Na_2As_4O_{11}$ and $NaAs_3O_8$, were also reported to melt incongruently [13]. All works measured the melting temperatures using DTA, except for the work of Amadori [21] who measured the melting temperatures using an alternative technique, hereon called the Current Method (CM). It may be briefly summarized as the following: attaching the sample to two wires, it is used to complete a circuit. Upon heating, the electrical signal will drop (or cease) due to the deformation of the sample causing a loss of contact between sample and circuitry. The change in signal is used to indicate melting temperature. A summary of the melting temperatures may be seen in Table 4.1. The melting point of $NaAsO_3$ was reported with relative agreement in the studies as 600 ^oC (873 K) [21] to 615 ^oC (888 K) [20,21]. $Na_4As_2O_7$ varied a little more melting from 815 ^oC (1088 K) [23] up to 845 ^oC (1118 K) [21], 847 ^oC (1120 K) [24] and 850 ^oC (1123 K) [22]. The differences between the multiple works for the two compounds are very small, aside from the measurement of $Na_4As_2O_7$ by Buketov et al. [23] and may be owed to experimental errors as the experimental set up between each work was similar. Except for the work

of Leung and Calvo [24], in each work, the experiments were conducted using non-sealed corundum crucibles. Leung and Calvo [24] do not indicate what crucible may have been used when conducting their experiments, however, they prepared their sample of $Na_4As_2O_7$ by heating a hydrated form, $Na_2HAsO_4 \cdot 7H_2O$ to approximately 900 ^oC. Amadori [21] prepared samples by mixing a stoichiometric ratio of As_2O_5 and Na_3AsO_4. Isabaev et al. [22] mixed stoichiometric ratios of As_2O_5 and Na_2O and annealed for over 200 hours. Buketov et al. [23] conducted their experiments using the compound in their hydrated states, NaH_2AsO_4 and Na_2HAsO_4. The larger difference observed by Buketov et al. [23] may be owed to their use of beginning their experiment with the hydrated compounds. As the sample was heated it would slowly dehydrate and the water loss would lead to early loss in mass and may reduce the sensitivity of the measurement, resulting in inaccurate values. This becomes particularly apparent when examining Na_3AsO_4, as the melting temperature was reportedly much greater. The melting temperature of Na_3AsO_4 varied considerably amongst the works. Values of 1000 ^oC (1273 K) [23] to 1260 ^oC (1533 K) [19,20] were measured. Again, the differing result of Buketov et al. [23] may be attributed to the fact they began their experiment with a hydrated compound, $Na_3AsO_4 \cdot 12H_2O$. Coursol et al. [25] measured a melting point of 1390 ^oC (1663 K) using DTA, but after conducting another experiment where pure Na_3AsO_4 was equilibrated up to 1400 ^oC (1673 K) and quenched, there was no liquid phase found. The difference in results was attributed to the fact that Al_2O_3 crucibles were used for DTA, leading to contamination due to the high temperatures, whereas sealed Pt capsules were used for the equilibration and quench. Using alternative phase diagrams ($Na_3AsO_4 - Ca_3(AsO_4)_2$ and $Na_3AsO_4 - Na_2SO_4$), Coursol et al. [25] extrapolated the melting temperature of Na_3AsO_4 to be 1430 ^oC (1703 K). While the work of Coursol et al. [25] appears rigorous and difficult to refute, the melting temperature measured by Amadori [21] and Isabaev et al. [22] were considered for the

optimization. The work by Amadori [21] and Isabaev et al. [22] are not as thoroughly explained, however, the work done appears reasonable and consistent among most of the works, though, this does not prove that their results are necessarily correct. $Na_5As_3O_{10}$ reportedly melted incongruently into solid $Na_4As_2O_7$ and liquid solution at 680 ^oC (953 K) [22] to 697 ^oC (970 K) [21]. The remaining compounds, $Na_2As_4O_{11}$ and $NaAs_3O_8$, were both reported to melt incongruently. $Na_2As_4O_{11}$ formed solid As_2O_5 and liquid at 670 ^oC (943 K) and $NaAs_3O_8$ decomposed to form solid As_2O_5 and $Na_2As_4O_{11}$ at 600 ^oC (873 K)[13]. Kasenov et al. [13] prepared their samples by mixing stoichiometric ratios of As_2O_5 and $NaAsO_3$. As_2O_5 was prepared by oxidizing arsenic with H_2O_2 and $NaAsO_3$ by mixing Na_2CO_3 with As_2O_5. There is no mention of the samples being annealed, however, they were sealed in quartz ampoules.

Phase diagram measurements of the liquidus were studied in several works [11,19,20,24]. Amongst the multiple works, enough data was available to produce a composite phase diagram containing experimental data at all compositions. A plot of the experimental phase diagram points of measurement are presented in Figure 4.1, superimposed upon the final optimized phase diagram. Information regarding the literature data will be discussed further in this section while the optimization will be discussed in later sections (Section 4.2). Measurements were made using DTA except for the work of Amadori [21], using the previously mentioned alternative technique of CM. Measurements of the liquidus curve were made in intervals from multiple studies: from 0 to 0.25 mole fraction of As_2O_5 [26], 0.25 to 0.5 [22], 0.25 to 0.6 [21] and 0.5 to 1.0 [13]. It should be noted that the measurements by Buketov et al. [26] from 0 to 0.25 mole fraction of As_2O_5 were conducted using Na_2CO_3 rather than Na_2O, as such the data here is considered unreliable. Regions where there were overlapping sets of experimental investigations show good agreement between the multiple works (0.25 to 0.6). Furthermore, while large portions of the phase diagram were reported

to be investigated by a single author (0 to 0.25, 0.6 to 1.0) the data appear to have good agreement at the bordering compositions (0.25, 0.5/0.6).

4.1.2 Thermodynamic Properties

Enthalpy of formation measurements were found for $Na_4As_2O_7$ (- 2413.8±6.6 kJ mol^{-1}) [27], Na_3AsO_4 (-1550.058±5 kJ mol^{-1}) [28], $Na_2As_4O_{11}$ (-2702.4±6.7 kJ mol^{-1})[29] and $NaAs_3O_8$ (-1836±7.5 kJ mol^{-1}) [29]. These values are presented on an oxide basis, that is the resulting value is solely from the reaction of the two constituents. Measurements were made using solution calorimetry with a 1:4000 $AgNO_3$ solution [25,27] and bomb calorimetry [28]. A summary of the enthalpies of formation obtained from literature may be seen in Table 4.2. In Figure 4.2, a plot of experimental enthalpies of formation depending on composition may be seen, along with the optimized enthalpy of formation curve. This optimization will be discussed further in later sections. There were no investigations where the standard entropy of any compound was directly measured. Heat capacity measurements were available for $NaAsO_3$ [30], $Na_4As_2O_7$ [31], Na_3AsO_4 [31] and $Na_5As_3O_{10}$ [31]. These were measured by dynamic calorimetry using an IT-S-400 calorimeter. Dynamic calorimetry is when a sample is rapidly heated over a wide temperature range, where the heat supplied, and the sample temperature are constantly monitored [32]. When the power used to heat the sample is much greater than the heat loss from the sample, the instantaneous heating rate will depend on the supplied power and the heat capacity of the sample. This type of calorimetry is particularly useful for dealing with unstable samples, such as evaporation or decomposition, both of which are major concerns when dealing with Na_2O and As_2O_5. Figures 4.3 to 4.6 contain plots of the measured heat capacity data. Superimposed on the data are heat capacity functions that have been fitted. The fitting of Na_3AsO_4 was done by Coursol

et al. [25]. Table 4.3 contains a summary of the heat capacity functions fitted to the available literature data.

There were no studies that measured the standard entropy of any of the six compounds.

4.2 Thermodynamic Optimization

4.2.1 The Gibbs Energies of Stoichiometric Compounds

$Na_4As_2O_7$ and Na_3AsO_4 were the only compounds where both enthalpy of formation [25,26] and heat capacity measurements [31] were reported in literature. For $Na_2As_4O_{11}$ and $NaAs_3O_8$, experimental data was limited to only enthalpy of formation [29], whereas $NaAsO_3$ and $Na_5As_3O_{10}$ were limited to only heat capacity data [28,29]. As thermodynamic data were limited, values found in literature were taken as is when conducting their optimization. When adjusting the values, all adjustments were made so that they remained within the reported error ranges. One exception to this was the enthalpy of formation of Na_3AsO_4. Coursol et al. [25] had previously optimized this compound and the enthalpy was optimized using the work and evaluation of others [26,31,32].

Na_3AsO_4 was optimized in a previous study by Coursol et al., [25] and all the thermodynamic properties were taken directly from their work. The Neumann-Kopp rule is an empirical estimation method where it has been found to predict the heat capacities of mixed oxides at room temperature with a high-degree of accuracy [35]. That is to say, the heat capacity of a binary compound may be calculated as the sum of the heat capacities of its constituents. It should be mentioned, however, that the heat capacity determined using the Neumann-Kopp rule is found to deviate at higher temperatures [35]. Molar heat capacity may be expressed as the sum of different sources of contribution, such as vibrational, molar volumetric, magnetic, vacancies and others [35].

Significant to all compounds are vibrational and volumetric contributions [35]. The molar volume of the compound will change with increasing temperature and this will be a source of change in heat capacity at higher temperatures [35]. While this is not the only source of deviation, it is a significant source of deviation and part of the reason why the Neumann-Kopp rule deviates at higher temperatures [35]. At room temperature, however, the deviations due to temperature are not significant. The entropy values of the compounds were taken directly to be calculated by the Neumann-Kopp rule using the binary constituents as they provide a good base in the complete absence of experimental entropy data. Furthermore, the change in standard entropy is relatively small, restricting deviations in the Gibbs free energy to higher temperatures. The heat capacities of the two oxide components, the Na_3AsO_4 and As_2O_5 were used for the Neumann-Kopp rule instead of those of Na_2O and As_2O_5. Since Na_3AsO_4 is the most stable compound in this binary system, taking the heat capacity of Na_3AsO_4 for the Neumann-Kopp rule reduces the number of parameters to estimate the Gibbs energy of a compound between the two constituents. By doing so, this applies a constraint on the heat capacity and entropy, thus resulting in the enthalpy of formation becoming a model parameter to be optimized. Table 4.4 contains a summary of the enthalpies of formation (expressed as enthalpy of reaction, further details seen in the table). These values are the one obtained after the final optimization. Details as to how they were obtained are outlined in the following section. Figure 4.7 shows a plot of the optimized entropy of formation depending on the composition.

4.2.2 The Gibbs Energy of Liquids

In order to model Na_2O – As_2O_5 system the coordination number of the two constituents needed to be determined. As it was mentioned Section 2.1.2, the coordination number determines the

composition of the maximum short-range ordering. For this reason, the coordination number of O^{2-} was determined previously [36] by introducing $\Delta g_{AB} = -\infty$ in the Si-O binary system, as the configurational entropy should approach to zero at the composition of $X_O = \frac{1}{3}$. Since the coordination number of an ion must be proportional to its charge number (z_i), the coordination number of a cation (Z_{cat}) was determined by the charge ratio between the cation and oxygen incorporated with the pre-determined coordination number of oxygen ($Z_{cat} = \frac{z_i}{2} Z_{O^{2-}}$). According to the phase diagram, the maximum short-range ordering composition lies at 0.25 mole fraction As_2O_5, seen in the form as the Na_3AsO_4 compound with its high melting point, implying the composition with the minimum Gibbs free energy of this in this system. As such, a coordination ratio of 1:3 of Na_2O:As_2O_5 appears ideal. To achieve this ideal coordination ratio while being consistent with charge proportionality, the cation of As^{5+} was modified to AsO^{3+}. This modification must also be and is consistent with the ideal coordination ratio of the other arsenic-containing systems investigated in this work: CaO – As_2O_5 and MgO – As_2O_5. This is of particular importance when producing a larger multi-component database, as consistency among the end members is necessary to produce a proper self-consistent database.

Having defined coordination ratio to be consistent with the composition of 0.25 mole fraction As_2O_5, it is important that the liquidus curve be fitted to well-reproduce the Na_3AsO_4 melting temperature. This was done by using the g^{00} liquid solution parameter as this parameter has the strongest effect on all parts of the liquidus curve and will define the overall shape. When examining the liquidus from 0.25 to 0.3, the curve drops sharply. In order to fit this, a strict set of parameters were required to recreate this. As the region from 0.25 to 0.5 had relatively more thermodynamic data, there were fewer degrees of freedom when fixing the curve. Further adjusting and fixing the liquidus from 0.3 to 0.6 was controlled by the addition of the g^{01} parameter. This parameter has

greater influence on the As_2O_5 rich side, as such, it may be used with minimal effect on the Na_2O rich side of the phase diagram. Reproducing the data from 0.6 to 1.0 proved to be very challenging to reproduce. The modification of this region was controlled by the contributions of a third solution parameter, g^{04}. This parameter has such a significantly greater effect on the As_2O_5 rich side of the phase diagram that the changes brought by it modify only very high As_2O_5 regions. The unknown enthalpies of compounds were initialized using the Neumann-Kopp rule and adjusted to help fit the liquidus curve, but care was taken to not adjust them too much. A summary of the solution parameters used to optimize the liquidus may be seen in Table 4.5.

4.2.3 Results and Discussion

When examining the calculated phase diagram, the poor fit from 0 to 0.25 mole fraction As_2O_5 is highly apparent. This is because the authors who investigated that region [26], used Na_2CO_3 instead of Na_2O and their reported melting temperature of Na_2O is consistent with that of Na_2CO_3 [37]. As such, priority to reproduce the data in that region of the phase diagram was reduced. The parameter that affects this region of the phase diagram is only the g^{00} parameter. The g^{00} parameter has a symmetric effect centered around the composition of maximum short-range ordering. However, the two other parameters used, g^{01} and g^{04}, do not affect the phase diagram from 0 to 0.25 and affect only from 0.25 to 1.0. As such, the additional two parameters were used to further fix the phase diagram from 0.25 onwards. Much care was taken when fitting the liquidus curve from 0.25 to 0.5 as there were multiple studies [19,20] that had investigated this region using differing methods and producing consistent results. Also, highly apparent, is the poor fitting from 0.66 to 1.0. This is likely due to experimental challenges when dealing with the As_2O_5-rich region as As_2O_5 is a highly volatile and hygroscopic compound. The possibility of hydration increases

along with the likelihood of vaporization of As_2O_5 (or Na_2O as it is also volatile). It should be noted that the plotted experimental points [13] strongly suggest the existence of a miscibility curve due to its elongated shape, however, this elongated shape may also be produced by the volatilization of As_2O_5, causing the composition of the experiment to shift. A summary of the optimized parameters of the Na_2O – As_2O_5 system may be seen in Table 4.6.

5. Critical Evaluation and Thermodynamic Optimization of the $CaO - As_2O_5$ System

5.1 Literature Review

5.1.1 Phase Diagram Data

Four compounds were reported to exist in the $CaO - As_2O_5$ binary system: $CaAs_2O_6$ (CA), $Ca_2As_2O_7$ (C_2A), $Ca_3As_2O_8$ (C_3A) and $Ca_4As_2O_9$ (C_4A).

Apart from $Ca_3As_2O_8$, the melting temperatures of all the compounds had been studied by Kasenov et al. [14] using DTA. In addition to their work, further studies were available for $CaAs_2O_6$ [40], by DTA as well, and $Ca_4As_2O_9$ [39], by equilibration followed by quenching. For the remaining compound, the melting temperature of $Ca_3As_2O_6$ was measured by Guerin [40]. In this work, the cone fusion method was used to determine the melting point. The cone fusion method is where the sample is molded into the shape of a cone (sometimes a cube) and heated. The point at which the shape of the sample begins to deform is taken as the melting temperature. A solid-solid equilibration experiment was conducted by Coursol et al. [41] from approximately 0.19 to 0.24 mole fraction As_2O_5. A summary of the melting temperatures may be seen in Table 5.1. Further details about the information are discussed below. The melting point of $CaAs_2O_6$ was reported with direct agreement between the studies, with values of 850 ^oC (1123 K) [42] and 890 ^oC (1163 K) [14]. Found to melt incongruently, it was reported to decompose to $Ca_2As_2O_7$ and As_2O_5. Makhmetov et al. prepared their samples, by mixing molar ratios of calcium hydroxide, $Ca(OH)_2$, and 80% arsenious acid, $As(OH)_3$, where the remaining 20% is H_2O from a water bath. Samples were heated at 80 – 90 ^oC until a homogenous mass was formed then subsequently dried at 100 ^oC. Samples were prepared using porcelain basins, so it is likely that DTA experiments were

conducted using porcelain as well. Kasenov et al. [14] created As_2O_5 by mixing As with hydrogen peroxide. This was mixed with CaO and heated to 400 – 450 ^oC for 300 hours in quartz tubes. DTA was conducted using evacuated quartz ampoules. $Ca_2As_2O_7$ was reported to decompose at 1090 ^oC (1363 K) into $Ca_3As_2O_8$ and As_2O_5 [14]. $Ca_4As_2O_7$ was also reported to melt incongruently, however, between the studies, there was very little agreement [12,37]. Decomposing into $Ca_3As_2O_8$ and CaO, Kasenov et al. [14] reported the change to occur at 1250 ^oC (1523 K), whereas the work of Bauer and Balz [39] reported the compound to remain stable up to 1600 ^oC (it should be noted that the wording used to report their information was rather ambiguous. Stating: "…[$Ca_4As_2O_9$] can safely heat to 1600 ^oC (1873 K), it is unclear if it was intended to mean that the compound becomes unstable beyond the reported temperature or that they did not measure beyond it.). Bauer and Balz [39] prepared their sample by mixing $CaCO_3$ and As_2O_3 in nitric acid. This mixture was heated to 1200 ^oC for 20 hours. Additionally, a solid-solid equilibration experiment conducted by Coursol et al. [41] also showed no formation of liquid at 1400 ^oC (1673 K) at this composition either. Coursol et al.[41] conducted this experiment using sealed platinum capsules and heating for 24 hours, after which they were quenched in water. Kasenov et al.[14] does not provide a detailed explanation for their experimental methodology, but the remainder of their data appears consistent with the works of others. As such, the CaO used may have been contaminated, resulting in lower temperatures and errors that are apparent only at high CaO content compositions. The result of Bauer and Balz [39] is much more probable considering the high melting temperature of CaO and the high CaO content of the compound. $Ca_3As_2O_8$ was the only compound reported to melt congruently at 1450 ^oC (1723 K) [40]. The experiments by Guerin [40] were performed by placing the samples inside a platinum basket inside

a quartz tube. The tube is placed in a furnace with nitrogen circulating through it. How the sample was prepared was not mentioned in the presented or related works [43].

Phase diagram measurements of the liquidus were conducted by Kasenov et al. [14]. A plot of the experimental phase diagram points of measurement are presented in Figure 5.1, superimposed upon the final optimized phase diagram. Information regarding the literature data will be discussed further in this section while the optimization will be discussed in a later section (Section 5.2). The data points were measured by means of DTA using quartz ampoules. However, aside from 0.1 mole fraction As_2O_5 there no measurements of the liquidus curve from 0 to 0.2 and 0.25 to 0.55 reported by them. Additionally, Kasenov et al. [14] were unable to determine the melting point of $Ca_3As_2O_8$ due to the bursting of their vessels and instead cited literature [40]. It is unclear how they were unable to measure the melting of $Ca_3As_2O_8$ but were able to measure the liquidus at 0.1 mole fraction As_2O_5. It is unlikely that $CaCO_3$ was used instead of CaO, like the previous system. If this $CaCO_3$ were used, then Kasenov et al. [14] would likely have reported a completed (albeit shifted lower) phase diagram as the melting point of $CaCO_3$ is considerably lower. In the small measured region between $Ca_3As_2O_8$ and $Ca_4As_2O_9$, they report a two-phase region being composed of CaO and liquid. This is not possible, however, as CaO is not either one of the two components in this region. Their presented data implies the existence of some type of three-phase region that should be composed of $Ca_3As_2O_8$, $Ca_4As_2O_9$ and liquid. It is difficult to say exactly what the cause of this discrepancy may be, but it may be said that data reported between 0.2 – 0.25 mole fraction are not reliable.

5.1.2 Thermodynamic Properties

Experimental thermodynamic data was very limited for this system and measurements were reported only for $Ca_3As_2O_8$. In the NBS Technical Note, the enthalpy of formation was reported to be -3298.7 kJ mol^{-1} and the standard entropy was 225.936 J mol^{-1} K^{-1} [10]. It is not specified how these values were determined, however, the NBS Technical Note is a source that follows a series of high standards and ensures consistency amongst tabulated values.

5.2 Thermodynamic Optimization

5.2.1 The Gibbs Energies of Stoichiometric Compounds

As experimental thermodynamic was limited, most thermodynamic properties had to be estimated. $Ca_3As_2O_8$ had been previously optimized by Coursol et al. in their investigation [41], where enthalpy of formation and the standard entropy of this compound were initially reported to be evaluated by Barin [44] using the data of Wagman et al. [10]. There were no measurements reported for heat capacity, but it had been estimated by Barin. Table 5.2 shows the heat capacity reported by Barin [44] and the estimated Gibbs energy of fusion of $Ca_3As_2O_8$. For the remaining three compounds ($CaAs_2O_6$, $Ca_2As_2O_7$ and $Ca_4As_2O_9$), the heat capacities and standard entropies were estimated using the Neumann-Kopp rule. Estimation for the enthalpies of formation were initialized using the Neumann-Kopp rule and slightly adjusted in order to reproduce the reported data. The estimation of standard entropy and enthalpy of formation were done using the known values for $Ca_3As_2O_8$ and As_2O_5, so the change in enthalpy and entropy due to the reaction are not 0 J mol^{-1} and 0 J mol^{-1} K^{-1}. A summary of the optimized enthalpy of formation may be seen in

Table 5.3 and Figure 5.2 depicts a plot of the enthalpy of formation depending on composition. Figure 5.3 shows a plot of the entropy of formation depending on the composition.

5.2.2 The Gibbs Energy of Liquids

The main interaction parameter in liquid phase, g^{00} was estimated by Richard's rule. First, the Richard's rule was used to estimate the entropy of fusion of $Ca_3As_2O_8$, which states that the entropy of fusion is approximately 2.2 cal mol^{-1} K^{-1} for metals [45]. To use Richard's rule, it is vital to properly define the independent components in the liquid phase as this will ultimately define the entropy of fusion. At the outset, it may seem obvious to define the molecules to be all the individual elements composing the compound. That is, three Ca, two As and eight O for a total of 13 independent components mixing in liquid $Ca_3As_2O_8$. However, for this to be true, these independent components must be randomly distributed in the melt, but it is unlikely due to charge neutrality. Considering charge neutrality, the independent components are more likely to be CaO and $AsO_{2.5}$. This results in a total of five independent components. By describing the solution as such a mixture, the entropy of fusion is estimated to be 46.02 J mol^{-1} K^{-1}. Then, the g^{00} parameter was optimized to reproduce the estimated entropy of fusion of $Ca_3As_2O_8$ at its melting point. The overall liquidus shape was determined by the g^{00} parameter; additional parameters were used to make minor adjustment. This optimization result supports the phase transition temperature of $Ca_4As_2O_9$ measured by Bauer and Balz [39], resolving the discrepancy among experimental data [12,37,39].

5.2.3 Results and Discussion

As it was previously mentioned, the g^{00} parameter requires a strict set of values in order to properly reproduce the estimated entropy of fusion, fixing it. The only experimental data remaining is only phase diagram data and unknown enthalpies of formation are adjusted in order to reproduce reported melting temperatures. There is a poor match from 0 to 0.25 mole fraction As_2O_5 in this system. Although it was mentioned that Kasenov et al. [14] did not measure the liquidus curve at all compositions, they proposed what the phase diagram may theoretically appear as, up to approximately 0.1 mole fraction As_2O_5. Their proposed diagram at high CaO content appears questionable. In this unmeasured liquidus region, the proposed phase diagram strongly implies a greatly underestimated melting temperature of CaO. Due to this underestimation and the fact that Kasenov et al. [14] reported a decomposition temperature of $Ca_4As_2O_9$ far lower than what Bauer and Balz [39] and Coursol et al. [41] report it to be stable at, it is possible that they faced contamination with their experiments. A summary of the optimized parameters of the $CaO - As_2O_5$ system may be seen in Table 5.5.

6. Critical Evaluation and Thermodynamic Optimization of the $MgO - As_2O_5$ system

6.1 Literature Review

6.1.1 Phase Diagram Data

Three compounds were reported to exist in the $MgO - As_2O_5$ binary system: $MgAs_2O_6$ (MA), $Mg_2As_2O_7$ (M_2A), and $Mg_3As_2O_8$ (M_3A). Both $MgAs_2O_6$ [13,44-47] and $Mg_2As_2O_7$ [13,44,46] were reported to decompose. Measurements were made using DTA [13,47] and TG [44-46]. While TG cannot measure solid to liquid phase transformations, the compounds decomposed into a solid and gas, as such the authors reported the decomposition temperature to be when the rate of mass change became significant. $Mg_3As_2O_8$ was reported to melt congruently from DTA measurements [15] and incongruently from studies using TG [46,48]. A summary of the melting temperatures may be seen in Table 6.1. Additional details are discussed below.

The decomposition temperature of $MgAs_2O_6$ reported amongst the multiple studies were not all in agreement. Values of 600 ^oC (873 K) [44-46], 780 ^oC (1053 K) [15] and 890 ^oC (1163 K) [49] were reported. The last value reported, 890 ^oC was mistakenly reported, as the value corresponds to the peak value measured by DTA. The onset value occurs at approximately 820 ^oC (1093 K) and was adjusted accordingly for the present work. This value has somewhat better agreement with the other reported high-temperature values. Investigations by DTA [13-47] reported the compound to decompose into $Mg_2As_2O_7$ and As_2O_5 whereas the works using TG [44-46] reported the As_2O_5 component to further decompose into As_4O_6 and O_2 gases. The decomposition temperature of $Mg_2As_2O_7$ was also reported with a split set of values of 800 ^oC (1073 K) [44,46] and 980 ^oC (1253 K) [15]. Similar to the previous compound, the experiment using DTA reported the compound to

decompose to $Mg_3As_2O_8$ and As_2O_5 and the ones using TG saw the As_2O_5 further decompose to As_4O_6 and O_2 gases. Behavior of heating $Mg_3As_2O_8$ was found to be even more discordant amongst the works. Through TG, it was reported to decompose into $Mg_2As_2O_7$ and MgO at a number of temperatures 1000 ^oC (1273 K) [50], 1100 ^oC (1373 K) [48]. DTA found the compound to melt congruently at 1350 ^oC (1623 K) [15]. In the case of each compound investigated, it can be seen that Mattrat and Guerin [48] consistently report lower melting and decomposition temperatures than Ashlyaeva et al. [15], along with the works of Guerin [46], Bastick et al. [47] and Guerin et al. [50] who also report lower temperatures. Upon a cursory glance, it appears that the experimental technique to measure the transition is the primary controlling factor, as experiments measured by TG report values consistent with one another, but also consistently much lower than those measured by DTA. Guerin [46] and Bastick et al. [47] do not clearly state all the experimental conditions, making it difficult to ascertain the veracity of their claims. Mattrat and Guerin [48] conducted experiments under constant vacuum conditions. This is likely to cause problems when dealing with volatile samples as they will be more prone to sublimating at lower temperatures. This is particularly evident when looking at the experimental results related to $Mg_3As_2O_8$. Through TG, the compound was reported to decompose, however, Ashlyaeva et al. [15] found the compound to congruently melt at a relatively higher temperature. Ashlyaeva et al. [15] prepared samples by mixing As_2O_5 with MgO and annealing them in quartz ampoules at 400 – 450 ^oC for 300 – 350 hours with repeated intermixing. Gorokhova et al. [49] prepared samples by mixing H_3AsO_4 with $C_6H_6MgO_7$ and calcining them at 350 ^oC. The conditions as to how the experiments were conducted were not specified, however, the application of the research was towards the firing of copper electrolytic sludge, so it may be assumed that the authors had used open, non-vacuum conditions.

Phase diagram measurements of the liquidus were conducted by Ashlyaeva et al. [15]. A plot of the experimental phase diagram points of measurement are presented in Figure 6.1, superimposed upon the final optimized phase diagram. The literature data will be discussed further in this section while the optimization will be discussed in a later section (Section 6.2). The data points were measured using DTA using quartz ampoules. Similar to the previous system, Ashlyaeva et al. [15] did not measure the liquidus at all compositions, failing to do so from 0 to 0.2 mole fraction As_2O_5, however, there is no mention as to why.

6.1.2 Thermodynamic Properties

Experimental thermodynamic data was very limited for this system and experimental data was found for $Mg_3As_2O_8$ only in the NBS Technical note. The enthalpy of formation was reported to be -3059.7 J mol^{-1} and the standard entropy was 225.1 J mol^{-1} K^{-1} [10]. As it was previously mentioned, it is not clearly known how the values of NBS Technical Note are determined, however, it is trusted as a reliable source.

6.2 Thermodynamic Optimization

6.2.1 The Gibbs Energies of Stoichiometric Compounds

As experimental thermodynamic data was very limited in this system as well, thermodynamic properties had to be estimated once again. $Mg_3As_2O_8$ was the only compound reported with experimental thermodynamic data, as such, the values of the enthalpy of formation, standard entropy and heat capacity. Similar to the compound $Ca_3As_2O_8$ of the CaO – As_2O_5 system, $Mg_3As_2O_8$ had also been evaluated by Barin [44] using the data of Wagman et al. [10]. Again, the

heat capacity was estimated by Barin [44] as well. These values were taken directly when applying them towards the optimization of the system. In order to determine the heat capacities of the compounds $Mg_2As_2O_7$ and $MgAs_2O_6$, the Neumann-Kopp rule was employed. The enthalpies of formation were estimated, after optimizing the Gibbs energy of liquid phase, to reproduce melting temperatures reported by Ashlyaeva et al. [15]. A summary of the optimized enthalpy of formation may be seen in Table 6.2 and Figure 6.2 depicts a plot of the enthalpy of formation depending on composition. Figure 6.3 shows a plot of the entropy of formation depending on the composition.

6.2.2 The Gibbs Energies of Liquids

Similar to the CaO-As_2O_5 system, the major parameter, g^{00} for the liquid phase was estimated by Richard's rule. The overall shape of the liquidus curve is essentially fixed by this parameter alone. The inclusion of additional parameters has only a small effect on the shape and only may be used to slightly adjust the liquidus curve. Since, according to literature, the other compounds, $MgAs_2O_6$ and $Mg_2As_2O_7$, decompose rather than melt, the shape of the liquidus curve is dictated solely by the solution parameters.

6.2.3 Results and Discussion

As it was outlined in the previous section, the MgO – As_2O_5 system was essentially optimized by simply fitting available data. In the entire diagram, there is only one fixed point: the melting point of $Mg_3As_2O_8$. Therefore, to validate the optimization, a more rigorous exercise must be demonstrated. To do so, two methods were examined. In one method, the thermodynamic behavior of the MgO – As_2O_5 system and its compounds were compared to that of CaO – As_2O_5 and the

corresponding compounds. This method was based on the premise that Mg and Ca are from the same group in the periodic table and are presumed to have a periodic trend. In the second method, taking available vapor pressure data found in literature, the compounds were tested to determine whether or not the estimated thermodynamic properties were consistent with the literature data. The first method is referred to as the "Relative Ratio" method and the second as "Vapor Pressure." Further detail of the two methods are as follows:

Relative Ratio with CaO-As_2O_5 System

To estimate the enthalpy of formation with more physical meaning, it was assumed that the MgO system will behave similarly to the CaO system. As both MgO and CaO are alkali earth oxides, it was assumed that a periodic trend exists between the two constituents and binary systems. Taking this assumption, a ratio was taken between the enthalpy of formation (on an oxide basis) between the $Mg_3As_2O_8$ and $Ca_3As_2O_8$ compounds (i.e. the only compounds with thermodynamic data available from literature of each respective system). This ratio was then taken and multiplied with the (oxide based) enthalpy of formation of the CaO system compounds. The values produced by this were added to the correlating compounds of the MgO system. Therefore, while the magnitude changes differed from compound to compound, the ratio of the enthalpy of formation of $Mg_2As_2O_7$ with $Ca_2As_2O_7$ and $MgAs_2O_6$ with $CaAs_2O_6$ were the same. Directly taking these values alone were almost able to reproduce the currently optimized phase diagram, that is to say, this method was very close to reproducing the enthalpies of formation obtained from fitting the phase diagram data. This high degree of precision implies that a periodic trend indeed exists. With the degree of success this method has demonstrated, it would be worthwhile to use this method to predict other systems within the periodic group or apply it to those in others where at least one system has been partially studied.

Vapor Pressure

Available were investigations into the dissociation pressure of all three MgO – As_2O_5 compounds. Using the equilibrium dew point method, the vapor pressure of $Mg_3As_2O_8$ was measured from 1274 – 1353 ^oC [15]. The vapor pressure of $Mg_2As_2O_7$ and $MgAs_2O_6$ were measured from 630 – 745 ^oC and 855 – 990 ^oC, respectively [51]. The investigations were conducted based on the phase diagram experiments of Ashlyaeva et al. [15]. When the compounds decomposed or melted to produce a liquid, the As_2O_5 is asserted to decompose into As_4O_6 gas and O_2 gas. Further detail about the decomposition reactions and the experimental vapor pressure data may be seen in Figures 6.4 – 6.6. Matched with each set of data are vapor pressure data produced by FactSage by using the optimized MgO – As_2O_5 database. The results show that the database is able reproduce the literature data of the $Mg_3As_2O_8$ compound very well and quite well for $MgAs_2O_6$. The database, however, deviated considerably more when reproducing the $Mg_2As_2O_7$ data. As the optimized database appears consistent with nearly all the other measured thermodynamic data, it is believed that the discrepancy may be due to an error in the $Mg_2As_2O_7$ vapor pressure measurement or methodology. Compared to an earlier work, Mustafin [51] reports nearly identical (in some instances exactly the same) results as Kasenov and Ashlyaeva [52] when $MgAs_2O_6$ is discussed, however, fairly differing results when discussing $Mg_2As_2O_7$.

A summary of the optimized parameters of the MgO – As_2O_5 system may be seen in Table 6.4.

7. Conclusion

Research was carried out to produce optimized thermodynamic databases for the arsenic-containing binary systems Na_2O – As_2O_5, CaO – As_2O_5, MgO – As_2O_5. The thermodynamic properties of As_2O_5 were first evaluated prior to the optimization of the systems. Literature was reviewed for experimental thermodynamic data and evaluated; however, an insufficient amount of data was found for each of the three systems. The Na_2O – As_2O_5 system contained the most amount of thermodynamic data and supplementing missing data by estimating with the Neumann-Kopp rule. The liquidus of this system was fixed by reproducing the complex shape of the experimental phase diagram data from 0.25 – 0.5 mole fraction As_2O_5. The CaO – As_2O_5 and MgO – As_2O_5 systems had a considerable lack of experimental thermodynamic data, where only one compound was known in each system. For the CaO – As_2O_5 system, taking the data of the known compound, $Ca_3As_2O_8$, unknown properties of compounds were estimated using the Neumann-Kopp rule. Richard's rule was used to estimate the Gibbs energy of fusion of $Ca_3As_2O_8$ to fix the liquidus curve. For the MgO – As_2O_5 system, thermodynamic properties were estimated in a similar manner as the CaO – As_2O_5 system. The results of the optimization of the MgO – As_2O_5 system were compared to those of the CaO – As_2O_5 system and were found to follow a periodic trend. The results were further validated with experimental vapor pressure data. These thermodynamic databases may be used to understand simple arsenic-containing binary systems, providing insight to simpler procedures or steps to a complex design.

Further development of additional arsenic-containing systems and of higher order multicomponent systems will provide even greater understanding of arsenic and how it may be sequestered in an efficient and safe manner. Future work requires more experimental investigations into the thermodynamic properties of the unknown stoichiometric compounds of the systems, particularly

those of $CaO - As_2O_5$ and $MgO - As_2O_5$, as they lack the most amount of data. Additionally, phase diagram measurements to verify the shape of the liquidus curve as well verifying the reported congruent and incongruent melting temperatures are necessary, as this will better constrain the Gibbs energy of the liquidus and improve the quality of the thermodynamic optimization.

References

[1] World Health Organization. (2018). Arsenic. https://www.who.int/news-room/fact-sheets/detail/arsenic

[2] Government of Canada. (2018). Giant Mine Remediation Project. https://www.aadnc-aandc.gc.ca/eng/1534860491275/1534860581017

[3] Berman, R. G.; Brown, T. H., Contributions to Mineralogy and Petrology (1985), 89(2-3),168-83.

[4] Mysen B. O., Structure and properties of silicate melts. Vol. 354. Amsterdam: Elsevier, 1988.

[5] Pelton A. D.; Degterov S. A.; Eriksson G.; Robelin C.; Dessureault Y., Metallurgical and Materials Transactions B (2000), 31 (4), 651-9.

[6] Pelton A.D.; Chartrand P., Metallurgical and Materials Transactions A (2001), 32, 1355-1360.

[7] Chartrand P.; Pelton A. D., Metallurgical and Materials Transactions A (2001), 32, 1397-1407.

[8] Pelton A. D.; Chartrand P.; Eriksson G., Metallurgical and Materials Transactions A (2001), 32(6), 1409-16.

[9] Kirk-Othmer Encyclopedia of Chemical Technology. 3rd ed., Volumes 1-26. New York, NY: John Wiley and Sons, 1978-1984., p. V13: 420, 1981.

[10] Wagman, D. D.; Evans, W. H.; Parker, V. B.; Halow, I.; Bailey, S. M.; Schumm, R. H., NBS Technical Note 270-. National Bureau of Standards, USA, 1968.

[11] Pankratz, L. B., Thermodynamic Properties of Elements and Oxides. Bureau of Mines, USA, 1982

[12] Anderson, C. T., Journal of the American Chemical Society (1930), 52 (6), 2296-300

[13] Kasenov, B. K.; Kuznetsov, Yu. M.; Mazhenov, N. A.; Beilina, A. Z.; Saduova, G. B., Zhurnal Neorganicheskoi Khimii (1987), 32(1), 184-7.

[14] Kasenov, B. K.; Ashlyaeva, I. V.; Beilina, A. Z., Doklady Akademii Nauk SSSR (1990), 314(2), 452-5.

[15] Ashlyaeva, I. V.; Kasenov, B. K.; Beilina, A. Z., Zhurnal Neorganicheskoi Khimii (1991), 36(4), 1074-7.

[16] Kasenov, B. K.; Kuznetsov, Yu. M., Russian Journal of Inorganic Chemistry (1988), 33 (5), 766-8.

[17] Kasenov, B. K.; Kuznetsov, Yu. M., Kompleksnoe Ispol'zovanie Mineral'nogo Syr'ya (1992), 10, 44-7.

[18] Kasenov B. K.; Kuznetsov Y. M., Inorganic Materials (1993) 29 (5), 837-40.

[19] Kasenov, B. K.; Ashlyaeva I. V., Zhurnal Neorganicheskoj Khimii (1993), 38 (8), 1414-5 (SrO)

[20] Vogel W., Glass chemistry. Springer Science & Business Media, 2012.

[21] Amadori, M., Atti ist. Veneto sci. let. arti (1914), Volume Date1913-1914, 73(II), 1665-78.

[22] Isabaev, S. M.; Zhambekov, M. I.; Kasenov, B. K., Zhurnal Neorganicheskoi Khimii (1976), 21(11), 3134-7.

[23] Buketov, E. A.; Polukarov, A. N.; Isabaev, S. M.; Zhambekov, M. I., Vestnik Akademii Nauk Kazakhskoi SSR (1973), 29(6), 30-3.

[24] Leung, K. Y.; Calvo, C., Canadian Journal of Chemistry (1973), 51, 2082-2088.

[25] Coursol, P.; Pelton, A. D.; Chartrand, P.; Zamalloa, M., Metallurgical and Materials Transactions B (2005), 36B (6), 825-836.

[26] Buketov E. A.; Kasenov B.K.; Pashinkin A.S.; Isabaev S.M.; Buketov, E. A., Phase Equilibria and Thermodynamic Properties of Alkali Metal Arsenates, Alma Ata, Nauka, 1985

[27] Bukharitsyn, V. O.; Kasenov, B. K., Vestnik Akademii Nauk Kazakhskoi SSR (1988), (5), 74-7.

[28] Kubaschewski, O.; Itagaki, K., Ber. Bunsenges. Phys. Chem. (1982) , 86, 191-193.

[29] Kasenov, B. K.; Mustafin, E. S.; Oralova, A. T., Zhurnal Neorganicheskoi Khimii (1994), 39(6), 985-6.

[30] Oskembekov, I. M.; Kasenov, B. K., Kompleksnoe Ispol'zovanie Mineral'nogo Syr'ya (2000), (2), 90-91.

[31] Sharipova, Z. M.; Kasenov, B. K.; Bukharitsyn, V. O., Zhurnal Fizicheskoi Khimii (1991), 65(5), 1408-10.

[32] Kraftmakher Y., European Journal of Physics (2007), 28 (2), 351-8.

[33] Mixter W.G., American Journal of Science (1909), 28 (164),103.

[34] Dougill S. B.; Jeffes J.H., Trans. Inst. Min. Metall. C. (1980), 89.

[35] Leitner J.; Voňka P.; Sedmidubský D.; Svoboda P., Thermochimica Acta (2010), 497 (1-2), 7-13.

[36] Blander M.; Pelton A. D., Argonne National Lab., IL, USA, 1983.

[37] Kim J. W.; Lee H. G., Metallurgical and materials transactions B (2001), 32 (1), 17-24.

[38] Makhmetov, M. Zh.; Gorokhova, L. G.; Chuprakov, V. I., Zhurnal Prikladnoi Khimii (Sankt-Peterburg, Russian Federation) (1979), 52(9), 2103-5.

[39] Bauer H.; Balz W., Z. Anorg. Allg. Chem., (1965), 340 (56), 225–31.

[40] Guerin H., Comptes rendus (1935), 200, 1210-2.

[41] Coursol, P.; Pelton, A. D.; Chartrand, P.; Zamalloa, M., Canadian metallurgical quarterly (2005), 44 (4), 547-54.

[42] Makhmetov, M.; Gorokhova L.; Chuprakov V., Journal of Applied Chemistry of the USSR (1979), 52 (9), 1985-7.

[43] Guerin H., Comptes rendus (1936), 201, 997-8

[44] Barin I., Thermochemical Data of Pure Substances, Federal Republic of Germany, VCH, Weinheim, 1995.

[45] Tiwari G. P., Metal Science (1978), 12 (7), 317-20.

[46] Guerin, H., Compt. rend. (1937), 204, 1740-1.

[47] Bastick, M.; Guerin, H.; Dutailly, L., Bulletin de la Societe Chimique de France (1959), 77-80.

[48] Mattrat, P.; Guerin, H., Bulletin de la Societe Chimique de France (1960), (No. 4), 601-9.

[49] Gorokhova, L. G.; Makhmetov, M. Zh.; Zhakupova, R. Zh, Kompleksnoe Ispol'zovanie Mineral'nogo Syr'ya (1981), (12), 67-9.

[50] Guerin, H.; Mattrat, P.; Ronis-Bernet, C., Bulletin de la Societe Chimique de France (1970), 11, 3895-6.

[51] Mustafin E.U., Bulletin of Karaganda University (2010), 58 (2), 32-6.

[52] Kasenov B. K.; Ashlyaeva I. V., Izv. universities of the USSR. Ser. Physical (1991), 5, 120-1.

[53] Science Education Resource Center at Carleton College. (2019). Experimental Petrology Machines. https://serc.carleton.edu/research_education/equilibria/machines.html

[54] C. W. Bale, E. Bélisle, P. Chartrand, S. A. Decterov, G. Eriksson, A.E. Gheribi, K. Hack, I. H. Jung, Y. B. Kang, J. Melançon, A. D. Pelton, S. Petersen, C. Robelin. J. Sangster and M-A. Van Ende, FactSage Thermochemical Software and Databases, 2010-2016, Calphad, vol. 54, pp 35-53, 2016 <www.factsage.com>

Appendix A – Tables and Figures

Table 3.1 Thermodynamic properties of As_2O_5 in literature, which are used in the optimization in this study. The C_P function was re-fit to smooth the function from low-temperature C_P to high-temperature C_P. The entropy of fusion was assumed to be the same as that of P_2O_5.

Thermodynamic Property	Value	Technique	Comment	Reference
ΔH^o_{298} (J mol^{-1})	-924869		NBS Technical Note	Wagman et al., 1968
S^o_{298} (J mol^{-1} K^{-1})	105.4	Adiabatic Calorimetry	NBS Technical Note	Wagman et al., 1968
C_P (J mol^{-1} K^{-1})	100.842768+ 0.115118576 T + 1656027.2 T^{-2} 221.886539+ 0.048524302 T + 244032.4814 T^{-2} - 2117.135063 T$^{-0.5}$	Estimated Estimated	Fitted Smoothed to include low C_P data	Pankratz, 1982 This work (including data from Anderson 1930)
ΔH^o_f (J mol^{-1})	31656.2	Estimated	$\Delta S^o_f x T_f$	This work
ΔS^o_f (J mol^{-1} K^{-1})	31.25	Estimated	ΔS^o_f of P_2O_5	This work

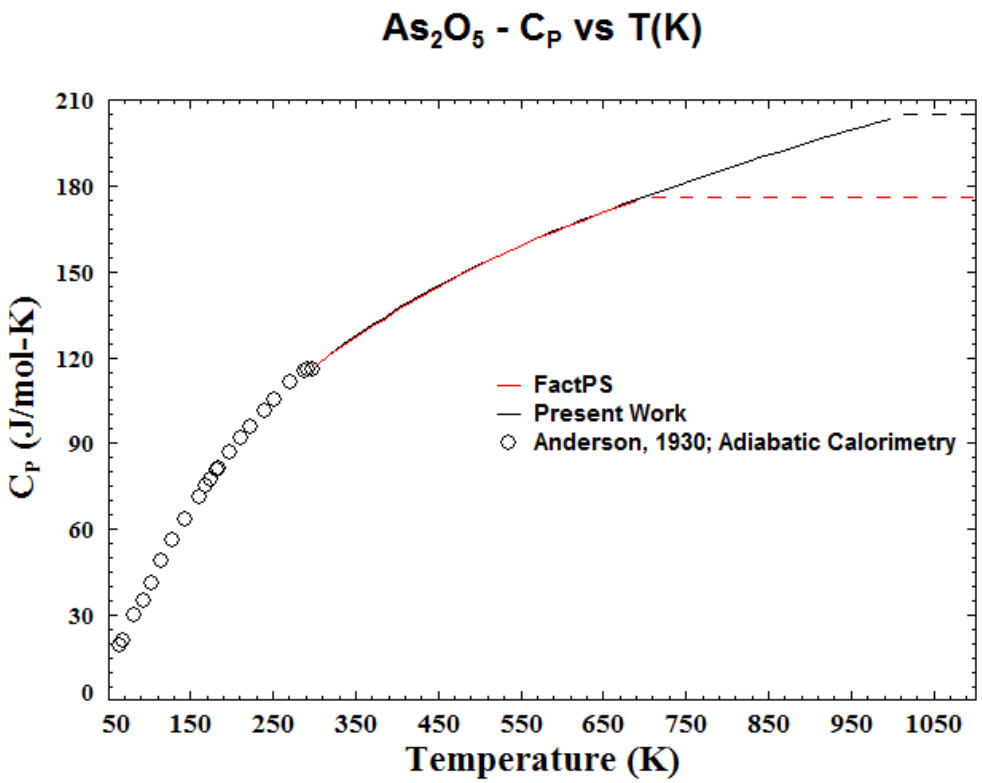

Figure 3.1 The C_P function of As_2O_5 along with the experimental C_p data at low temperature by Anderson [12].

Table 4.1 Invariant reactions in the Na_2O – As_2O_5 binary system.

Compound	Transition	Temperature [K (°C)]	Technique	Reference
NaAsO3 (NA)	$NaAsO_3$ → Liquid	873 (600) 888 (615) 888 (615)	CM* DTA DTA	Amadori, 1914 Buketov et al., 1973 Isabaev et al., 1976
Na4As2O7 (N2A)	$Na_4As_2O_7$ → Liquid	1118 (845) 1088 (815) 1123 (850) 1120 (847)	CM DTA DTA DTA	Amadori, 1914 Buketov et al., 1973 Isabaev et al., 1976 Leung and Calvo, 1973
Na3AsO4 (N3A)	Na_3AsO_4 → Liquid	1533 (1260) 1273 (1000) 1533 (1260) 1663 (1390)	CM DTA DTA DTA	Amadori, 1914 Buketov et al., 1973 Isabaev et al., 1976 Coursol et al., 2005a
Na5As3O10 (N5A3)	$Na_5As_3O_{10}$ → $NaAsO_3$(s) + $Na_4As_2O_7$(l)	970 (697) 953 (680)	CM DTA	Amadori, 1914 Isabaev et al., 1976
Na2As4O11 (NA2)	$Na_2As_4O_{11}$ → melt + As_2O_5(s)	943 (670)	DTA	Kasenov et al., 1987
NaAs3O8 (NA3)	$NaAs_3O_8$ → As_2O_5(s) + $Na_2As_4O_{11}$(s)	873 (600)	DTA	Kasenov et al., 1987

*** "Current Method, CM"** The sample is attached to two wires to complete a circuit. Upon heating, the electrical signal will drop (or cease) due to the deformation of the sample causing a loss of contact between sample and circuitry. The point at which the change in signal is measured is used to indicate the melting temperature.

Table 4.2 Summary of experimental standard enthalpy of formation of compounds in literature.

Compound	ΔH_{298} (kJ mol^{-1})	Technique	Reference
$NaAsO_3$ (NA)	-	-	-
$Na_4As_2O_7$ (N_2A)	-2413.8±6.6	Solution Calorimetry (1:4000 $AgNO_3$)	Bukharitsyn and Kasenov, 1988
Na_3AsO_4 (N_3A)	-1550.058±5 -1506.243	Bomb calorimetry	Kubashewski and Itagaki 1982 Coursol et al 2005a
$Na_5As_3O_{10}$ (N_5A_3)	-	-	-
$Na_2As_4O_{11}$ (NA_2)	-2702.4±6.7	Solution Calorimetry (1:4000 $AgNO_3$)	Kasenov et al 1994
$NaAs_3O_8$ (NA_3)	-1836±7.5	Solution Calorimetry (1:4000 $AgNO_3$)	Kasenov et al 1994

Table 4.3 Summary of experimental heat capacities of compounds in literature.

Compound	C_P (J mol^{-1} K^{-1})	Comment
$NaAsO_3$ (NA)	115.8 + 0.0281 T - 3358709.0 T^{-2} - 9.48E-6 T^2	Oskembekov and Kasenov, 2000
$Na_4As_2O_7$ (N_2A)	162.2 + 0.5619 T - 3625059.7 T^{-2} - 0.0003 T^2	Sharipova et al., 1991
Na_3AsO_4 (N_3A)	106.4 + 0.1832 T + 9E-5T^2	Coursol et al., 2005a; Sharipova et al., 1991
$Na_5As_3O_{10}$ (N_5A_3)	191.4 + 0.7172 T - 3707419.5 T^{-2} - 0.0003 T^2	Sharipova et al., 1991

Table 4.4 Table of enthalpies of reaction per mole of compound formed. These values were used to complete the optimization of the Na_2O – As_2O_5 binary system. Included is experimental data from literature and values calculated using the Neumann-Kopp rule to estimate compounds without literature data. Enthalpies of reaction available in literature were slightly adjusted within their reported error of measurement during the optimization. Estimated values were calculated using the enthalpy of Na_3AsO_4 and As_2O_5.

Compound	$\Delta H_{Reaction}$ (J/Reaction)	Comment
$NaAsO_3$ (NA)	-55000	1/3 Na_3AsO_4 + 1/3 As_2O_5 (Neumann-Kopp Rule)
$Na_4As_2O_7$ (N_2A)	-103036	Bukharitsyn and Kasenov, 1988
Na_3AsO_4 (N_3A)	0	Coursol et al., 2005a
$Na_5As_3O_{10}$ (N_5A_3)	-177000	5/3 Na_3AsO_4 + 2/3 As_2O_5 (Neumann-Kopp Rule)
$Na_2As_4O_{11}$ (NA_2)	-160810	Kasenov et al., 1994
$NaAs_3O_8$ (NA_3)	-93300	Kasenov et al., 1994

Table 4.5 Solution parameters used to optimize the Na_2O - As_2O_5 binary system.

Na_2O – As_2O_5 Solution Parameters (J/mole of pair)
$\Delta g^{00}_{Na,AsO/O}$ = -477561.6 + 46.024T
$\Delta g^{01}_{Na,AsO/O}$ = -296840 + 75.312T
$\Delta g^{04}_{Na,AsO/O}$ = -45000

Table 4.6 Summary of optimized parameters of the Na_2O – As_2O_5 system.

Liquid phase (Modified Quasichemical Model)				
Coordination numbers: $Z^{Na}_{NaNa} = 0.68872188, Z^{AsO}_{AsOAsO} = 1.37744376$ $\Delta g_{Na_2O-As_2O_5} = (-477561.6 + 46.024 \cdot T) + (-296840 + 75.312 \cdot T)X_{AsO-AsO} + (-45000)X^4_{AsO-AsO}$				
Stoichiometric compounds				
Phase	ΔH^o_{298K} (kJ mol^{-1})	S^o_{298K} (J mol^{-1}K^{-1})		Reference*
Na_2O(s1)	-417.982	75.061		[54]
Na_2O(s2)	-416.224	76.779		
Na_2O(s3)	-404.300	86.372		
Na_2O(l)	-356.602	120.320		
Na_3AsO_4	-1506.243	195.213		[25]
$Na_5As_3O_{10}$	-3303.984	345.808		Present Work
$Na_4As_2O_7$	-2419.650	255.559		[27]
$NaAsO_3$	-865.371	90.249		Present Work
$Na_2As_4O_{11}$	-2706.420	285.935		[29]
$NaAs_3O_8$	-1828.539	195.686		[29]
Phase	C_p (J mol^{-1} K^{-1})		Temperature (K)	Reference
Na_2O(s1)	66.22 + 0.0438T - 813370T^{-2} - 1.41T^2		298 - 1023	[54]
Na_2O(s2)	66.22 + 0.0438T - 813370T^{-2} - 1.41T^2		1023 - 1243	
Na_2O(s3)	66.22 + 0.0438T - 813370T^{-2} - 1.41T^2		1243 - 1405	
Na_2O(l)	104.6		T > 1405	
Na_3AsO_4	106.43 + 0.1832T + 9E-5 T^2		298-673	[25]
$Na_3AsO_{4(l)}$	270.48		T > 673	
$Na_5As_3O_{10}$	191.46 + 0.7172T - 3707419T^{-2} - 0.000348T^2		298 - 1013	[31]
$Na_4As_2O_7$	162.27 + 0.5619T - 3625059T^{-2} - 0.000273T^2		298 - 1013	[31]
$NaAsO_3$	115.76 + 0.0281T - 3358708T^{-2} - 9.48E-6 T^2		298 - 1013	[30]
$Na_2As_4O_{11}$	509.99 + 0.1409T - 325305T^{-2} - 1.41E-5 T^2 - 4234.27T$^{-0.5}$		298 - 1013	Neumann-Kopp
$NaAs_3O_8$	365.94 + 0.0947T – 40636.3T^{-2} - 7.04E-6 T^2 – 3175.7T$^{-0.5}$		298 - 1013	Neumann-Kopp

* ΔH^o_{298K} only, all S^o_{298K} were estimated using Neumann-Kopp

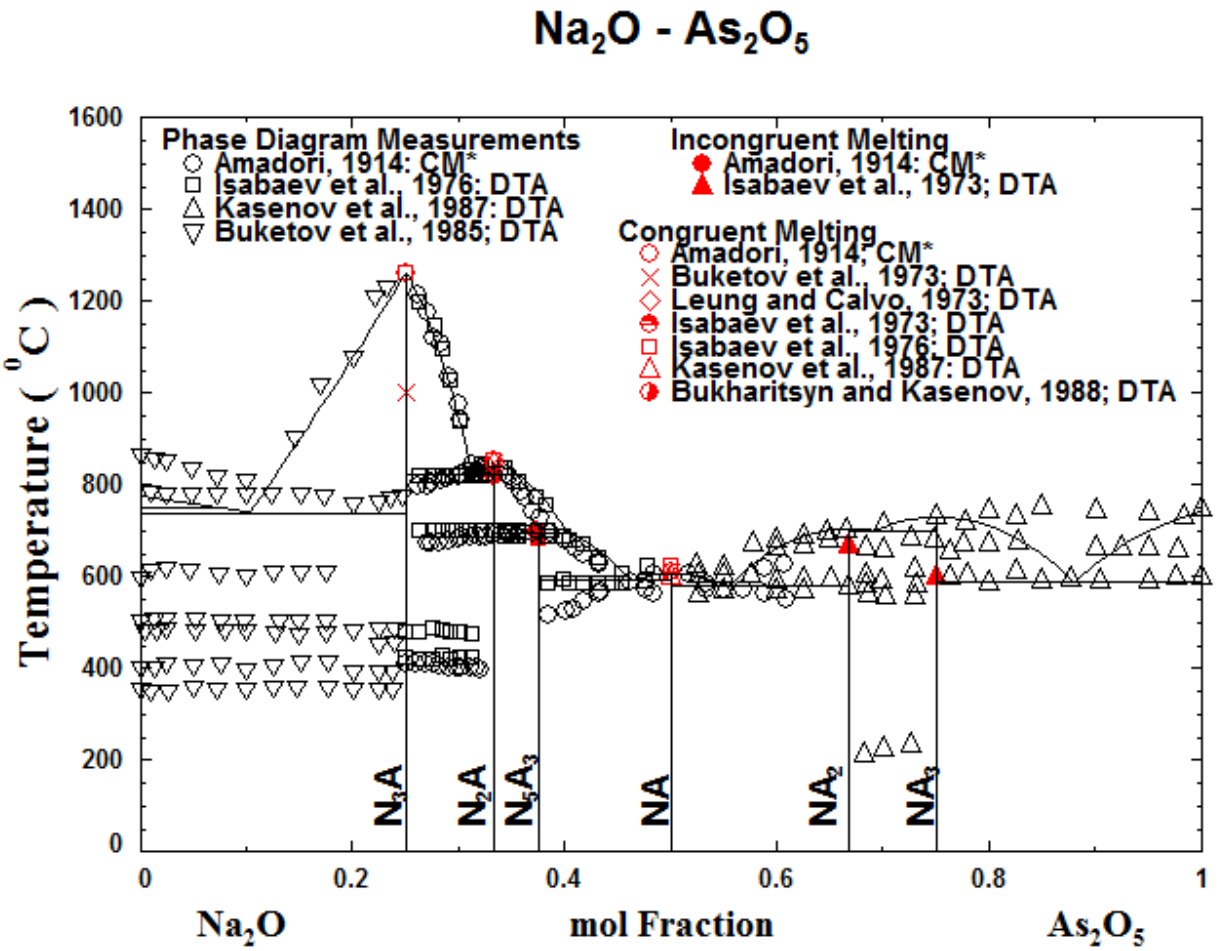

Figure 4.1 The optimized phase diagram of the Na_2O – As_2O_5 binary system along with relevant literature data. N and A in the compound names represent Na_2O and As_2O_5, respectively.

*** "Current Method, CM"** The sample is attached to two wires to complete a circuit. Upon heating, the electrical signal will drop (or cease) due to the deformation of the sample causing a loss of contact between sample and circuitry. The point at which the change in signal is measured is used to indicate the melting temperature.

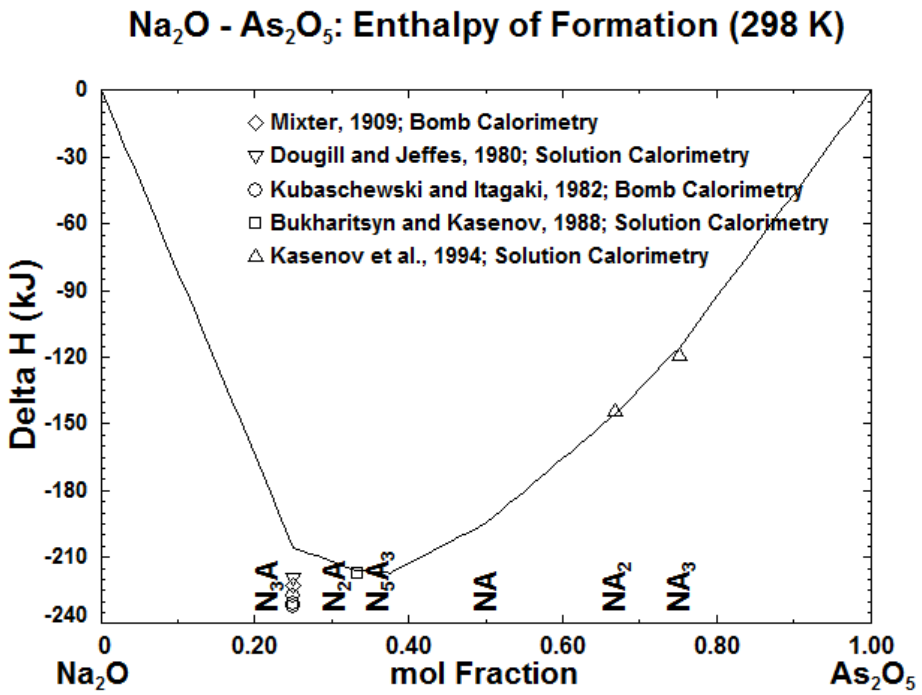

Figure 4.2 The optimized enthalpy of formation of the Na_2O – As_2O_5 system along with relevant literature data.

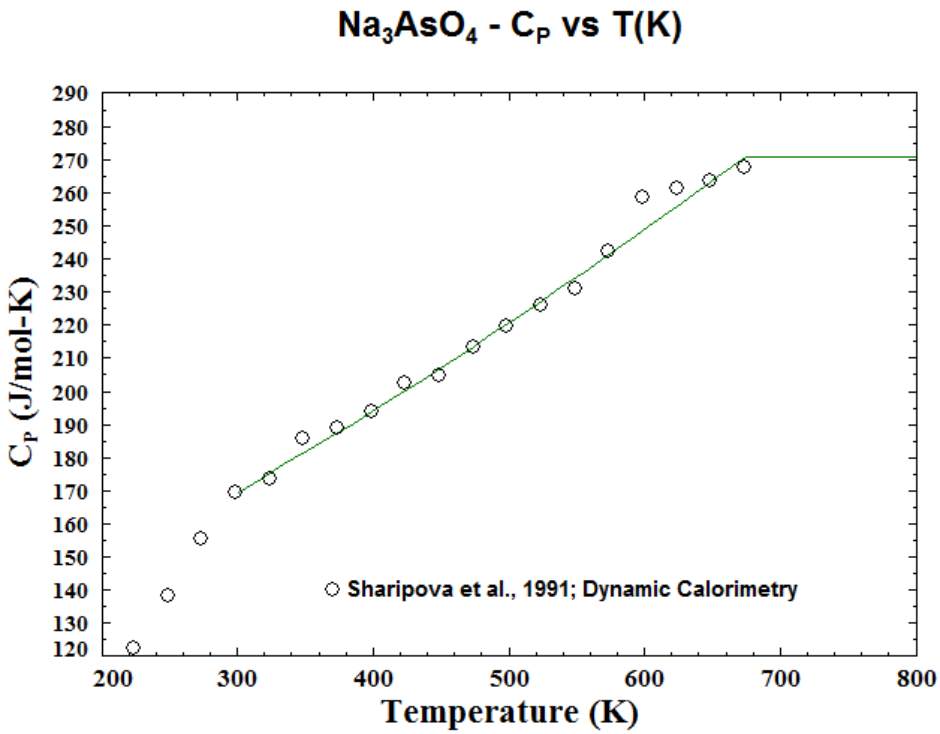

Figure 4.3 Optimized heat capacity of Na_3AsO_4 (originally established by Coursol et al. [25]) along with experimental data from Sharipova et al [31].

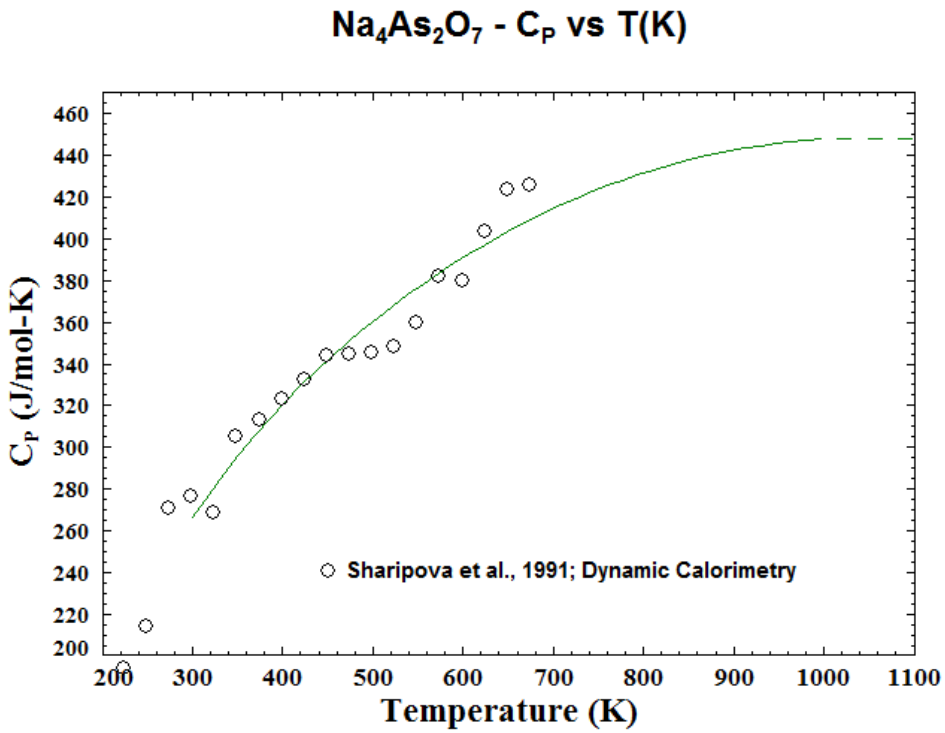

Figure 4.4 Optimized heat capacity of $Na_4As_2O_7$ along with experimental data from Sharipova et al [31].

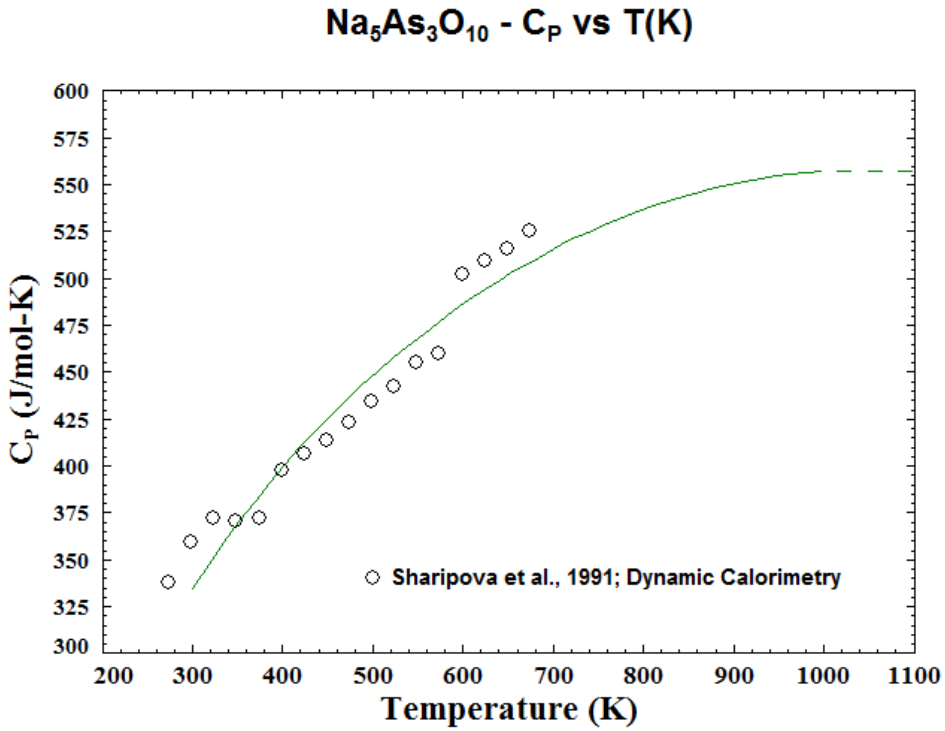

Figure 4.5 Optimized heat capacity of $Na_5As_3O_{10}$ along with experimental data from Sharipova et al [31].

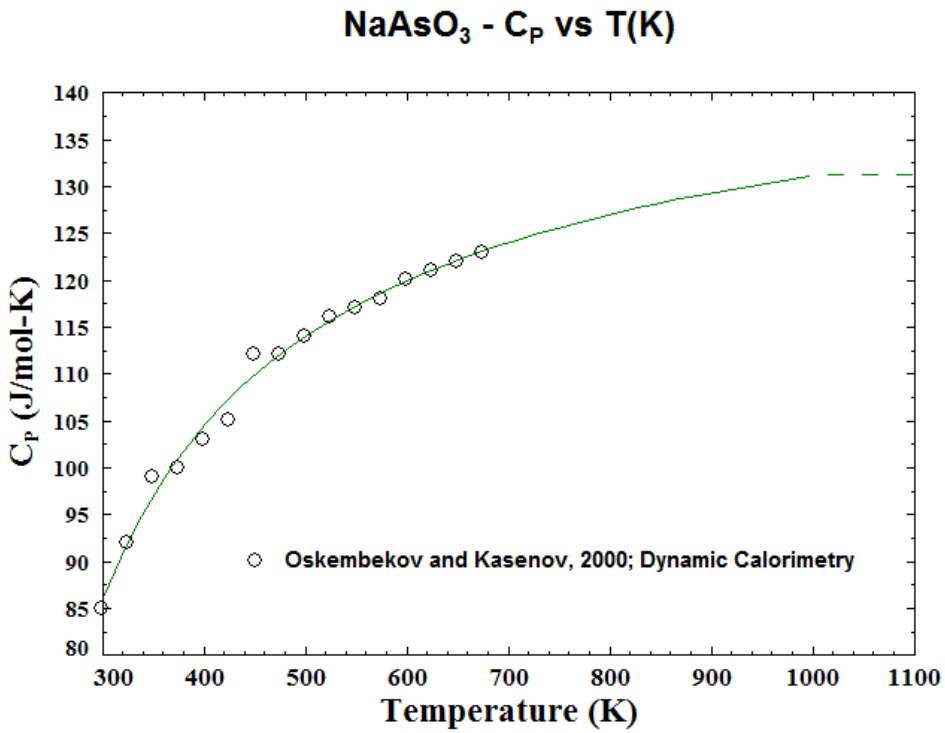

Figure 4.6 Optimized heat capacity of $NaAsO_3$ plotted along with experimental data from Oskembekov and Kasenov [30].

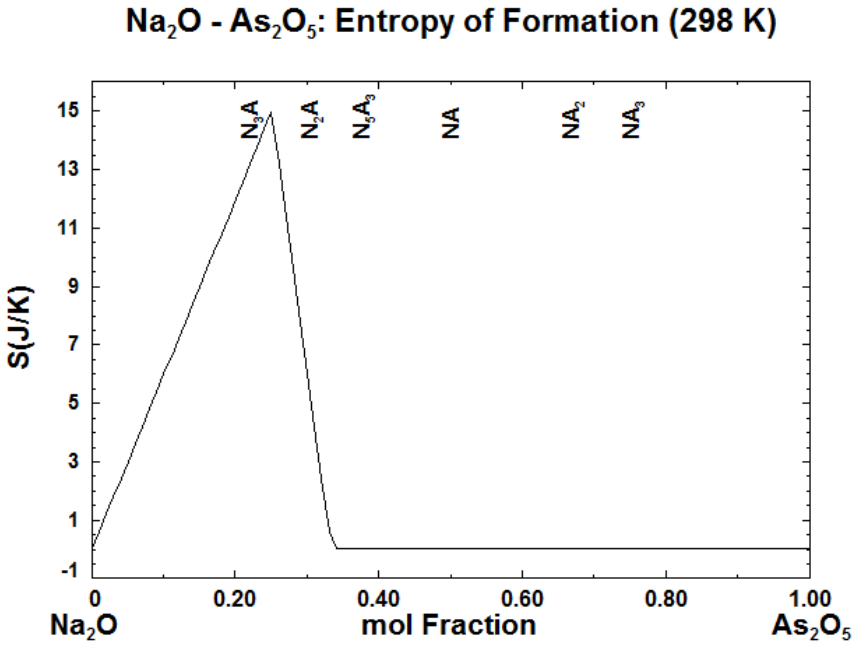

Figure 4.7 Calculated entropy of formation of the Na_2O – As_2O_5 system at 298 K.

Table 5.1 Invariant reactions in the CaO – As_2O_5 binary system.

Compound	Transition	Temperature [K (°C)]	Technique	Reference
$CaAs_2O_6$ (CA)	2 $CaAs_2O_6$ → $Ca_2As_2O_7$ + As_2O_5	1123 (850) 1163 (890)	DTA DTA	Makhmetov et al., 1979 Kasenov et al., 1990
$Ca_2As_2O_7$ (C_2A)	3 $Ca_2As_2O_7$ → 2 $Ca_3As_2O_8$ + As_2O_5	1363 (1090)	DTA	Kasenov et al., 1990
$Ca_3As_2O_8$ (C_3A)	$Ca_3As_2O_8$ → Liquid	1723 (1450)	Cone Fusion	Guerin, 1936
$Ca_4As_2O_9$ (C_4A)	$Ca_4As_2O_9$ → $Ca_3As_2O_8$ + CaO Stable*	1523 (1250) 1873 (1600)	DTA QM†	Kasenov et al., 1990 Bauer and Balz, 1965

***** The wording of this work is ambiguous: stated is that the compound may be safely heated to 1600 °C. It is not clear if the compound becomes unstable beyond that temperature or if the authors did not investigate any higher temperatures.

† QM – Quenching method

Table 5.2 Heat capacity data found in literature and the optimized Gibbs energy of fusion of $Ca_3As_2O_8$.

Property	$Ca_3As_2O_8$ (C_3A)	Comment
C_P (J mol^{-1} K^{-1})	280.3 + 0.0535 T - 4129489 T^{-2} - 6.407316E-10 T^2	Barin [44]
ΔG^0_{fusion} (J mol^{-1})	81338.3 – 46.02 T	Richard's Rule

Table 5.3 Table of enthalpies of reaction per mole of compound formed. No experimental data was found except for that of $Ca_3As_2O_8$. The Neumann-Kopp rule was employed to estimate the enthalpies of compounds with no data. Estimated values were calculated using the enthalpies of $Ca_3As_2O_8$ and As_2O_5.

Compound	$\Delta H_{Reaction}$ (J/Reaction)	Comment
$CaAs_2O_6$ (CA)	-7327.5	1/3 $Ca_3As_2O_8$ + 2/3 As_2O_5 (Neumann-Kopp Rule)
$Ca_2As_2O_7$ (C_2A)	-6779.3	2/3 $Ca_3As_2O_8$ + 1/3 As_2O_5 (Neumann-Kopp Rule)
$Ca_3As_2O_8$ (C_3A)	0	Coursol et al., 2005b
$Ca_4As_2O_9$ (C_4A)	-5749.2	$Ca_3As_2O_8$ + As_2O_5 (Neumann-Kopp Rule)

Table 5.4 Solution parameters used to optimize the CaO – As_2O_5 binary system.

CaO – As_2O_5 Solution Parameters (J/mole of pair)
$\Delta g^{00}_{Ca,AsO/O}$= -340102 + 51.14487T
$\Delta g^{01}_{Ca,AsO/O}$= 10000 + 8T
$\Delta g^{02}_{Ca,AsO/O}$= -4000

Table 5.5 Summary of optimized parameters of the CaO – As_2O_5 system.

Liquid phase (Modified Quasichemical Model)			
Coordination numbers: $Z^{Ca}_{CaCa} = 1.37744376, Z^{AsO}_{AsOAsO} = 1.37744376$			
$\Delta g_{CaO-As_2O_5} = (-340102 + 51.14487 \cdot T) + (10000 + 8 \cdot T)X_{AsO-AsO} + (-4000)X^2_{AsO-AsO}$			
Stoichiometric compounds			
Phase	ΔH^o_{298K} (kJ mol^{-1})	S^o_{298K} (J mol^{-1}K^{-1})	Reference*
CaO	-635.090	37.750	[54]
CaO(l)	-555.594	65.691	
$Ca_4As_2O_9$	-3939.546	263.686	Present Work
$Ca_3As_2O_8$	-3298.707	225.936	[10]
$Ca_3As_2O_{8(l)}$	ΔH_f =75088	ΔS_f =46.024	Richard's Rule
$Ca_2As_2O_7$	-2514.206	185.770	Present Work
$CaAs_2O_6$	-1723.475	145.603	Present Work
Phase	C_p (J mol^{-1} K^{-1})	Temperature (K)	Reference
CaO	58.79 - 1147146T^{-2} - 133.9T$^{-0.5}$ + 102978788T^{-3}	298 - 2845	[54]
	62.76	T > 2845	
CaO(l)	58.79 - 1147146T^{-2} - 133.9T$^{-0.5}$ + 102978788T^{-3}	298 - 2845	
	62.76	T > 2845	
$Ca_4As_2O_9$	481.29 - 1147146T^{-2} - 3102.9T$^{-0.5}$ + 102978788T^{-3}	298 - 700	Neumann-Kopp
	328.29 - 0.05942T - 1147146T^{-2} - 133.9T$^{-0.5}$ + 102978788T^{-3}	700 - 1900	
	441.19 - 1147146T^{-2} - 3102.9T$^{-0.5}$ + 102978788T^{-3}	1900 - 2845	
	445.158	T > 2845	
$Ca_3As_2O_8$	280.3 + 0.0535T - 4129489T^{-2} - 6.407E-10 T^2	298 - 700	[44]
$Ca_3As_2O_{8(l)}$	280.3 + 0.0535T - 4129489T^{-2} - 6.407E-10 T^2	T > 1767	
$Ca_2As_2O_7$	355.6 + 0.0162T + 81344T^{-2} - 2685.04T$^{-0.5}$	298 - 700	Neumann-Kopp
	253.63 + 0.0558T + 81344T^{-2} - 705.7T$^{-0.5}$	700 - 1013	
	247.9 + 0.0396T	T > 1013	
$CaAs_2O_6$	288.76 + 0.0323T + 162688T^{-2} - 2401.09T$^{-0.5}$	298 - 700	Neumann-Kopp
	237.76 + 0.0522T + 162688T^{-2} - 1411.42T$^{-0.5}$	700 - 1013	
	226.35 + 0.0198T	T > 1013	

* ΔH^o_{298K} only, all S^o_{298K} were estimated using Neumann-Kopp

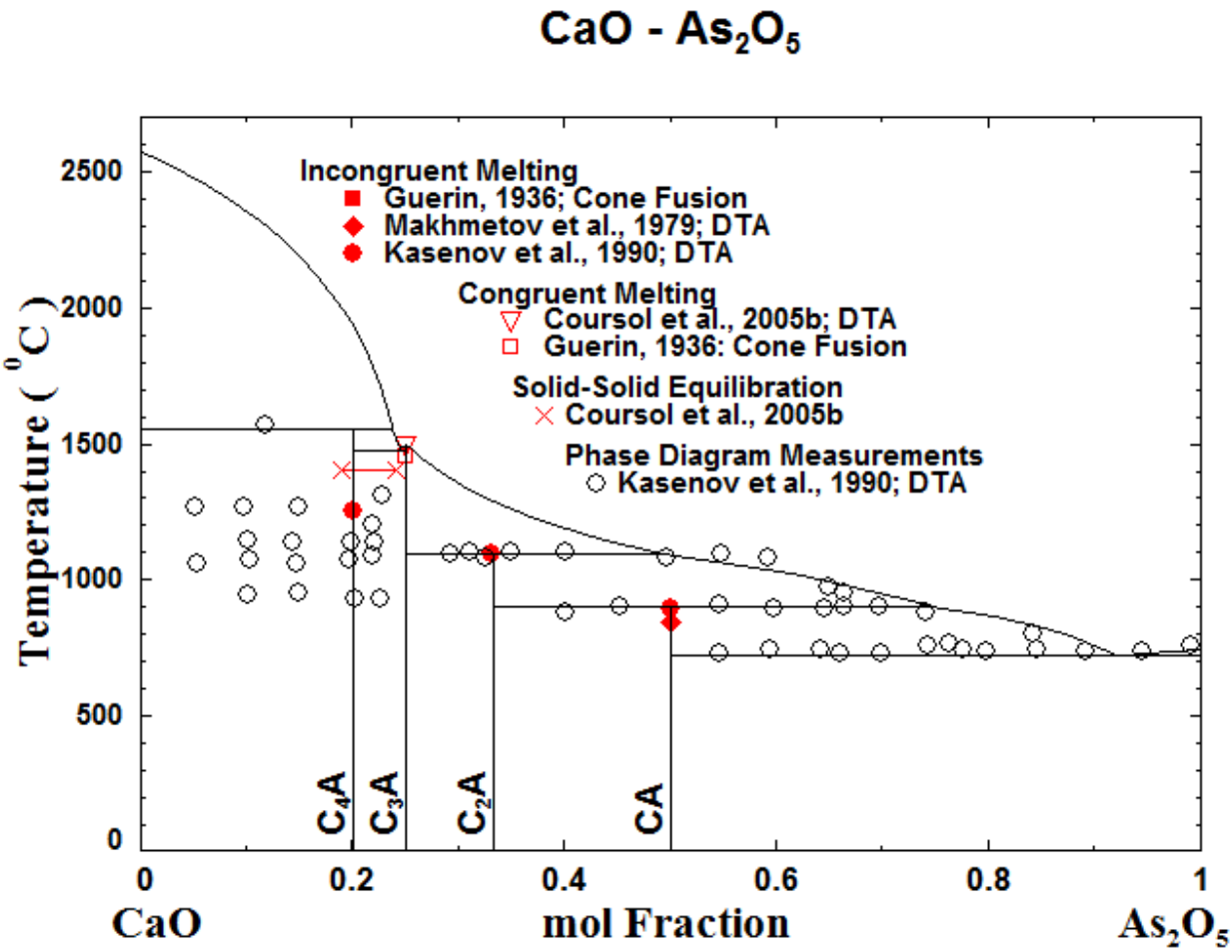

Figure 5.1 The optimized phase diagram of the CaO – As_2O_5 binary system plotted with relevant literature data. C and A in the compound names represent CaO and As_2O_5, respectively.

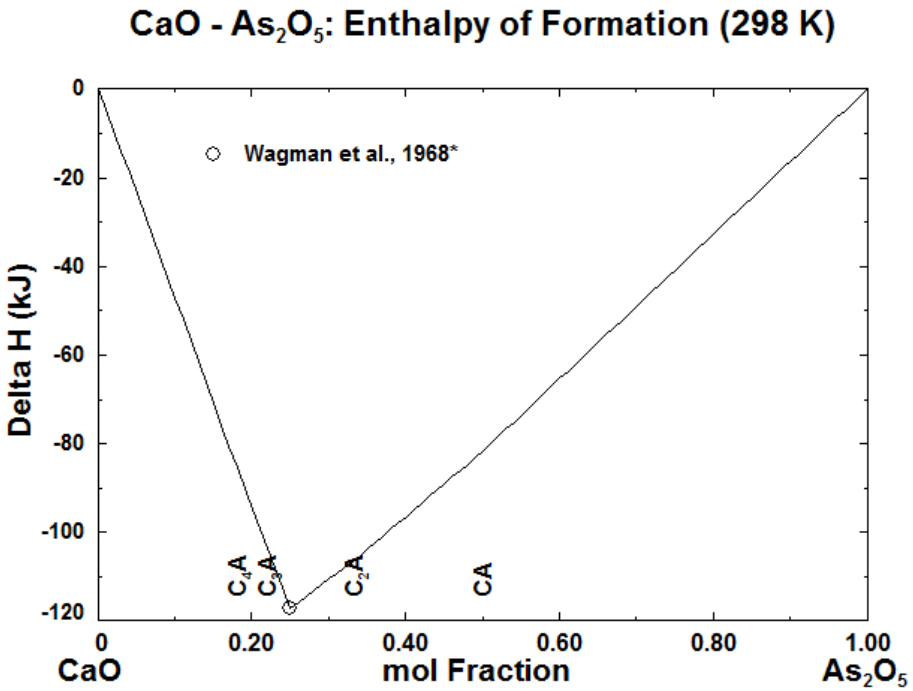

Figure 5.2 The optimized enthalpy of formation of the CaO – As_2O_5 binary system plotted with relevant literature data.

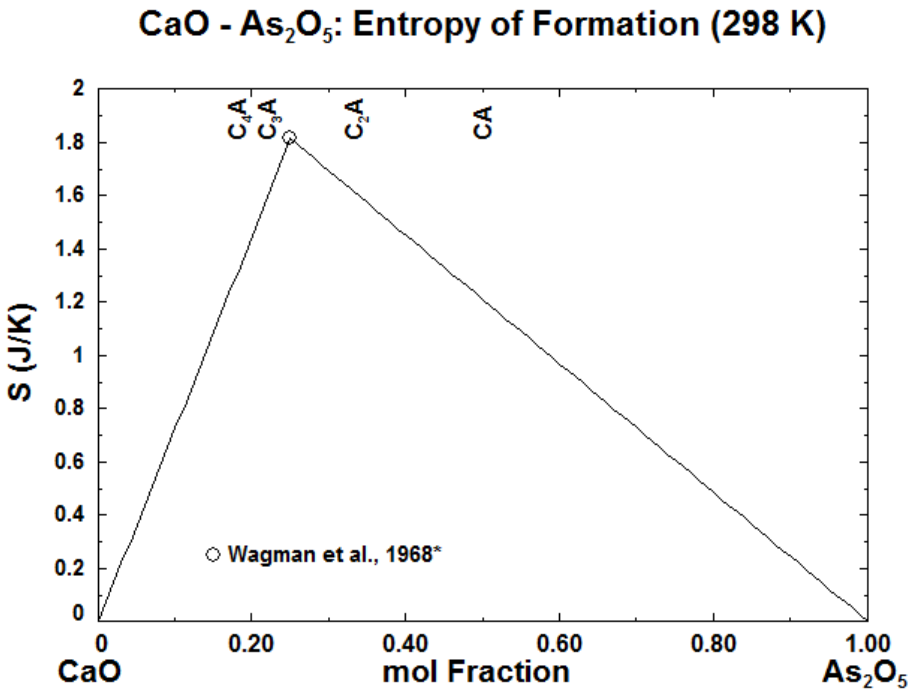

Figure 5.3 The optimized entropy of formation of the CaO – As_2O_5 binary system plotted with relevant literature data.

Table 6.1 Invariant reactions in the MgO – As_2O_5 binary system

Compound	Transition	Temperature [K (°C)]	Technique	Reference
$MgAs_2O_6$ (MA)	2 $MgAs_2O_6$ → $Mg_2As_2O_7$ + ½ $As_4O_{6\,(g)}$ + $O_{2\,(g)}$	873 (600)	TG	Guerin, 1937
		873 (600)	TG	Bastick et al., 1959
	2 $MgAs_2O_6$ → $Mg_2As_2O_7$ + As_2O_5	873 (600)	TG	Mattrat and Guerin, 1960
		1093 (820)*	DTA	Gorokhova et al., 1981
		1053 (780)	DTA	Ashlyaeva et al., 1991
$Mg_2As_2O_7$ (M_2A)	3 $Mg_2As_2O_7$ → 2 $Mg_3As_2O_8$ + ½ $As_4O_{6\,(g)}$ + $O_{2\,(g)}$	1073 (800)	TG	Guerin, 1937
		1073 (800)	TG	Mattrat and Guerin, 1960
	3 $Mg_2As_2O_7$ → 2 $Mg_3As_2O_8$ + As_2O_5	1253 (980)	DTA	Ashlyaeva et al., 1991
$Mg_3As_2O_8$ (M_3A)	$Mg_3As_2O_8$ → $Mg_2As_2O_7$ + MgO	1373 (1100)	TG	Mattrat and Guerin, 1960
		1273 (1000)	TG	Guerin et al., 1970
	$Mg_3As_2O_8$ → Liquid	1623 (1350)	DTA	Ashlyaeva et al., 1991

* The authors had originally reported 890 °C from their DTA measurements, however, they reported the peak values of the DTA curve and not the onset value. The value was approximately adjusted accordingly.

Table 6.2 Table of enthalpies of reaction per mole of compound formed. No experimental data was found except for that of $Mg_3As_2O_8$. The Neumann-Kopp rule was used to estimate the enthalpies of compounds with no data. Estimated values were calculated using the enthalpies of $Mg_3As_2O_8$.

Compound	$\Delta H_{Reaction}$ (J/Reaction)	Comment
$MgAs_2O_6$ (CA)	-5350.14	1/3 $Mg_3As_2O_8$ + 2/3 As_2O_5 (Neumann-Kopp Rule)
$Mg_2As_2O_7$ (C_2A)	-5086.64	2/3 $Mg_3As_2O_8$ + 1/3 As_2O_5 (Neumann-Kopp Rule)
$Mg_3As_2O_8$ (C_3A)	0	Barin, 1995

Table 6.3 Solution parameters used to optimize the MgO – As_2O_5 binary system.

MgO – As_2O_5 Solution Parameters (J/mole of pair)
$\Delta g^{00}_{Mg,AsO/O} = -255170 + 18.787T$
$\Delta g^{01}_{Mg,AsO/O} = 25000$
$\Delta g^{02}_{Mg,AsO/O} = -17000$

Table 6.4 Summary of optimized parameters of the MgO – As_2O_5 system.

Liquid phase (Modified Quasichemical Model)				
Coordination numbers: $Z^{Mg}_{MgMg} = 1.37744376, Z^{AsO}_{AsOAsO} = 1.37744376$ $\Delta g_{MgO-As_2O_5} = (-255170 + 18.787 \cdot T) + (25000)X_{AsO-AsO} + (-17000)X^2_{AsO-AsO}$				
Stoichiometric compounds				
Phase	ΔH^o_{298K} (kJ mol^{-1})	S^o_{298K} (J mol^{-1}K^{-1})		Reference*
MgO	-601.500	26.951		[54]
Mgo(l)	-545.345	27.004		
$Mg_3As_2O_8$	-3059.759	225.099		[10]
$Mg_3As_2O_{8(l)}$	ΔH_f =75088	ΔS_f =46.024		Richard's Rule
$Mg_2As_2O_7$	-2353.479	185.212		Present Work
$MgAs_2O_6$	-1641.586	145.324		Present Work
Phase	C_p (J mol^{-1} K^{-1})		Temperature (K)	Reference
MgO	61.11 - 621154T^{-2} - 296.2T$^{-0.5}$ + 5844612T^{-3}		298 - 3098	[54]
	66.944		T > 3098	
MgO(l)	72.80 - 0.0031T + 522751T^{-2} - 296.2T$^{-0.5}$ + 5844612T^{-3}		298 - 3098	
	66.944		T > 3098	
$Mg_3As_2O_8$	1059 + 0.318T - 8526T$^{-0.5}$ - 24.52T$^{0.5}$		298 - 1632	[44]
$Mg_3As_2O_{8(l)}$	1059 + 0.318T - 8526T$^{-0.5}$ - 24.52T$^{0.5}$		T > 1632	
$Mg_2As_2O_7$	779.9 + 0.228T + 81344T^{-2} - 6390T$^{-0.5}$ - 16.35T$^{0.5}$		298 - 1013	Neumann-Kopp
	774.3 + 0.212T - 5684T$^{-0.5}$ - 16.35T$^{0.5}$		1013 - 1400	
$MgAs_2O_6$	500.9 + 0.138T + 162688T^{-2} - 4253T$^{-0.5}$ - 8.173T$^{0.5}$		298 - 1013	Neumann-Kopp
	489.5 + 0.106T - 2842T$^{-0.5}$ - 8.173T$^{0.5}$		1013 - 1400	

* ΔH^o_{298K} only, all S^o_{298K} were estimated using Neumann-Kopp

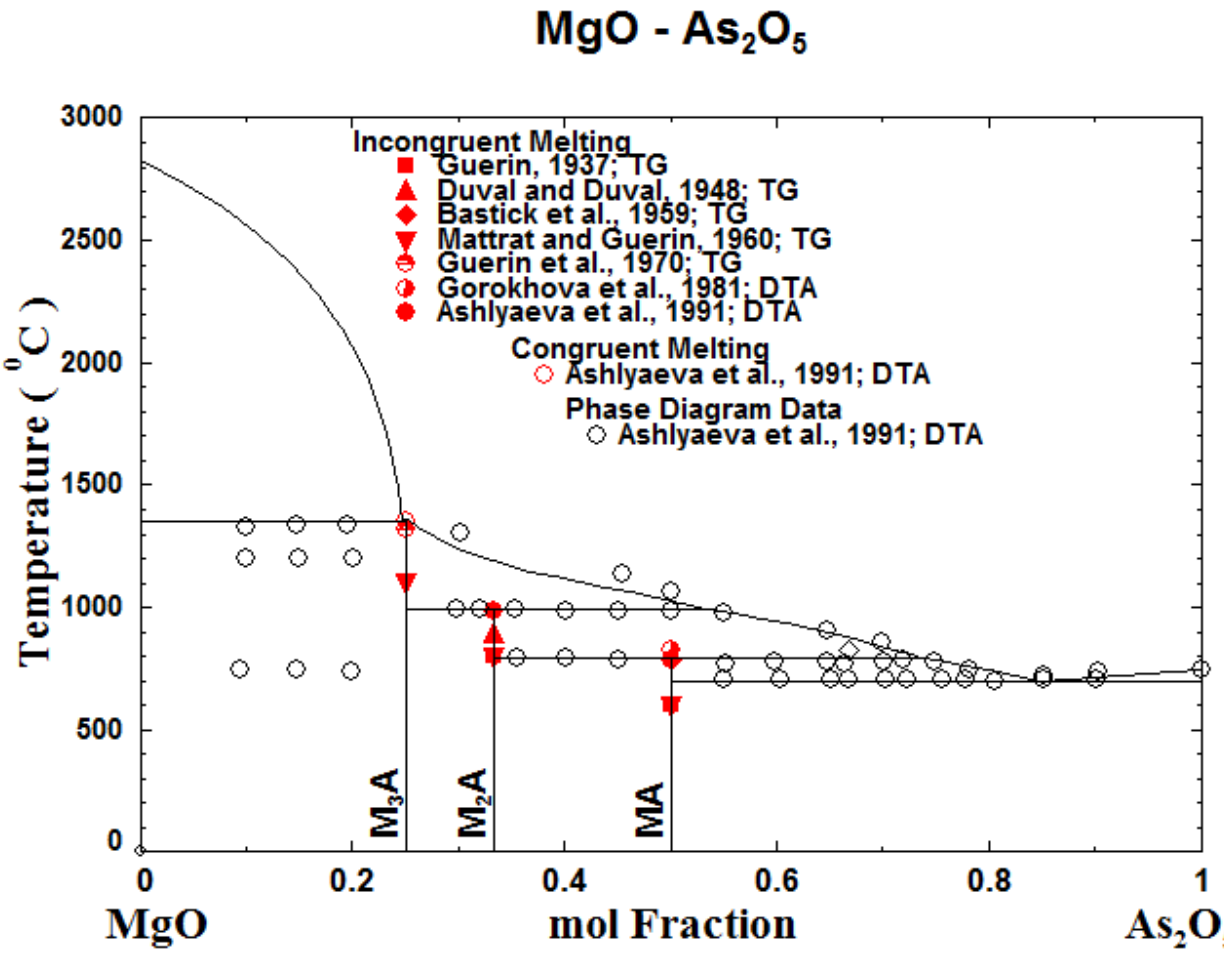

Figure 6.1 The optimized phase diagram of the MgO – As_2O_5 binary system plotted with relevant literature data. M and A in the compound names represent MgO and As_2O_5, respectively.

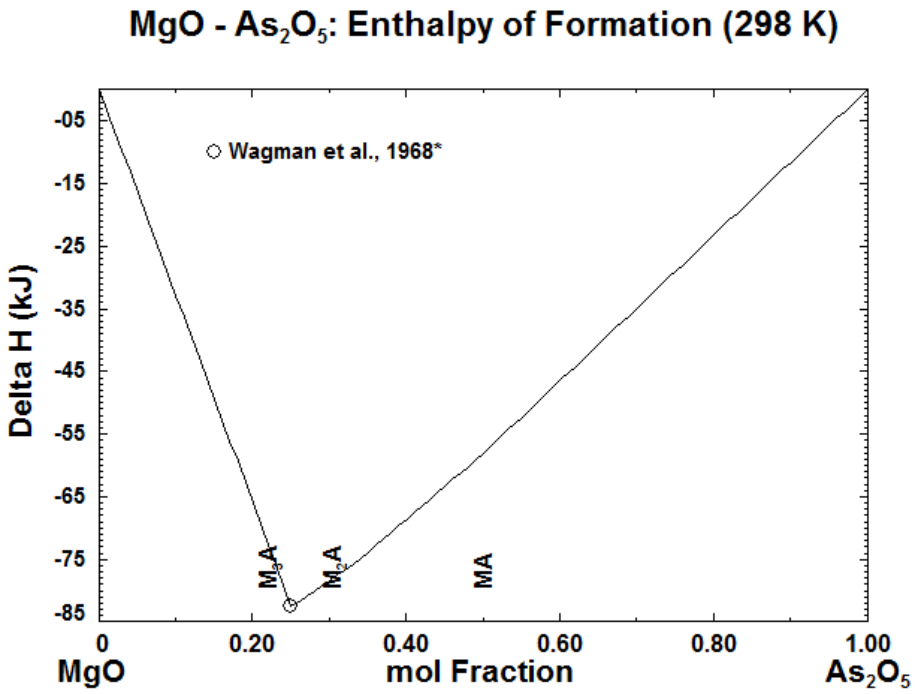

Figure 6.2 The optimized enthalpy of formation curve of the MgO – As_2O_5 binary system plotted with relevant literature data.

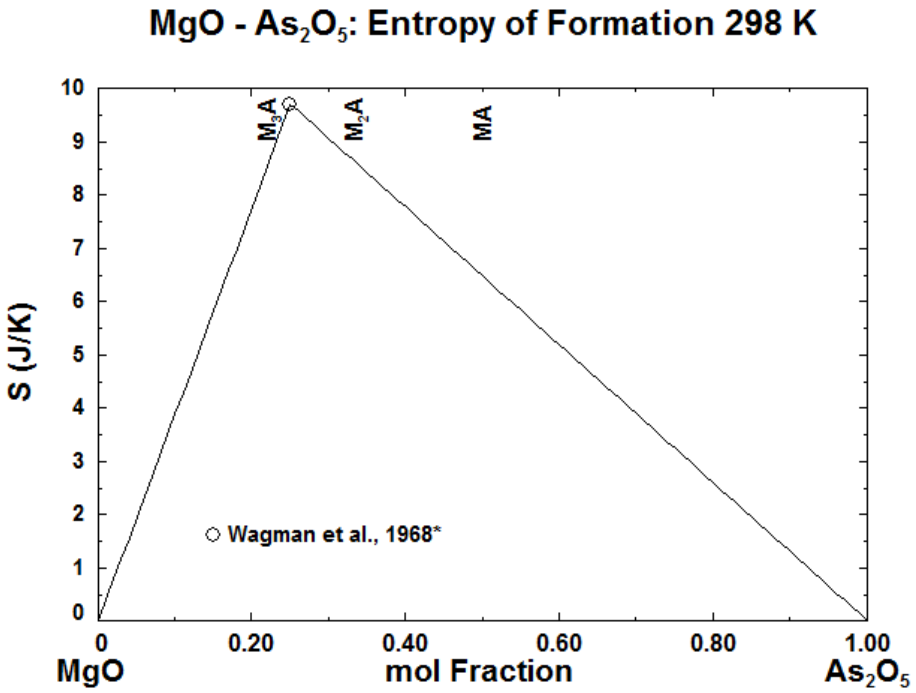

Figure 6.3 The optimized entropy of formation curve of the MgO – A_2O_5 binary system plotted with relevant literature data.

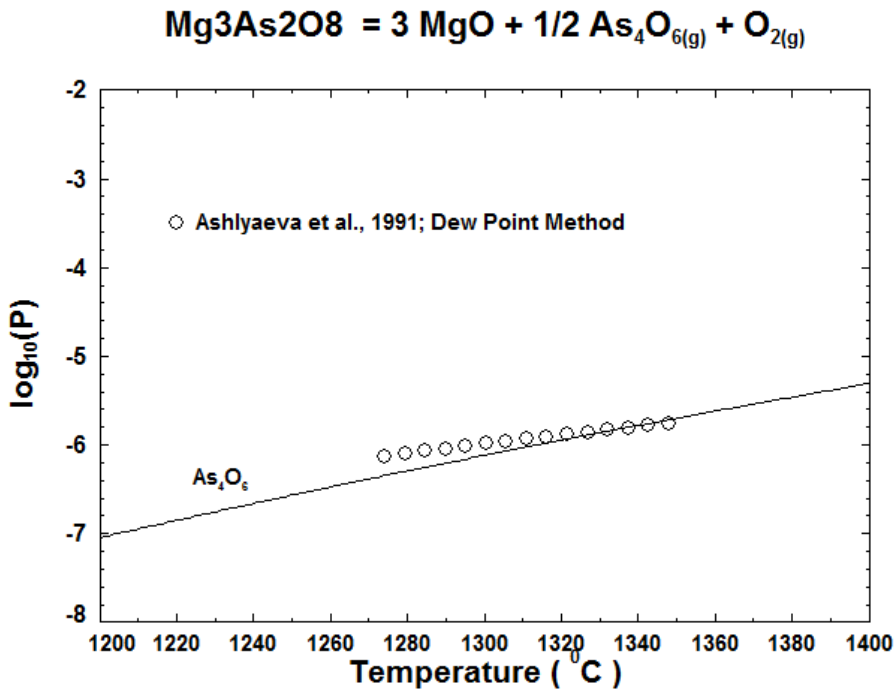

Figure 6.4 Vapor pressure of $Mg_3As_2O_8$ is calculated from the optimization of the MgO – As_2O_5 binary system. Plotted is relevant literature data of vapor pressure measurements.

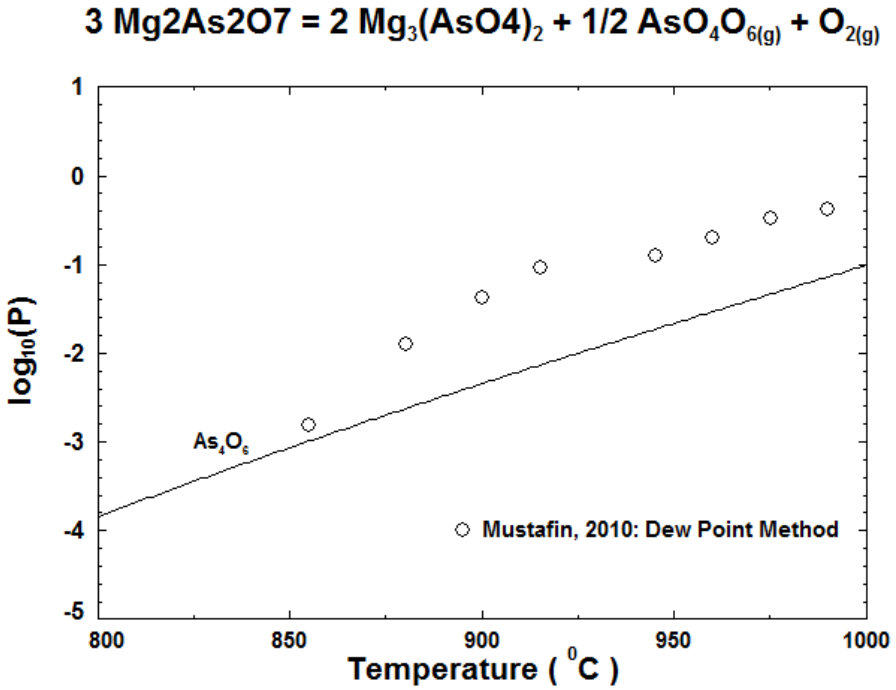

Figure 6.5 Vapor pressure of $Mg_2As_2O_7$ is calculated from the optimization of the MgO – As_2O_5 binary system. Plotted is relevant literature data of vapor pressure measurements.

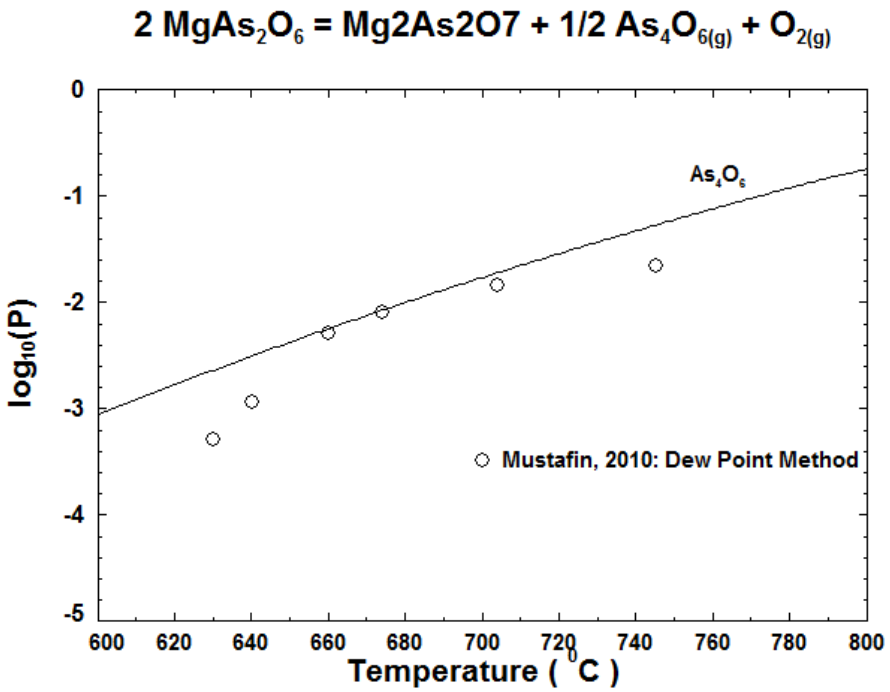

Figure 6.6 Vapor pressure of $MgAs_2O_8$ is calculated from the optimization of the MgO – As_2O_5 binary system. Plotted is relevant literature data of vapor pressure measurements.

Appendix B – Experimental Investigation: Methodology, Challenges and Future Considerations

B.1 Experimental Methodology

B.1.1 Materials and Sample Preparation

Mixtures for each system were prepared by mixing a stoichiometric ratio of MgO, CaO or Na_2O powder with As_2O_5 powder. The powdery mixtures were submerged under cyclohexane and, using a silica mortar and pestle, were mixed and grinded for one hour. This procedure was to ensure a homogenous mixture of the two constituents. The mixtures were submerged under cyclohexane to prevent moisture from the atmosphere being absorbed, due to the hygroscopic nature of As_2O_5. Due to the volatile nature of cyclohexane, the samples were mixed until most of the cyclohexane had evaporate. The resulting powdery mixtures were transferred to a small Pt dish. The mixtures were then dried in an oven at 433 ^oC to ensure no moisture for approximately 30 minutes. This temperature was chosen as preliminary investigations of As_2O_5 had indicated that any volatilization of As_2O_5 would be negligible while ensuring water removal. Mixture were transferred into vials sealed under Ar gas and the lids were tightly wrapped with parafilm when placed on standby. Samples were prepared once the mixtures were finished. The following compositions were prepared for both the CaO – As_2O_5 and MgO – As_2O_5 systems: 0.25, 0.33, 0.4, 0.5, and 0.6 mole fraction of As_2O_5. These compositions were chosen to confirm the shape of the liquidus and two phase regions (Figures 5.1 and 6.1).

Crucibles were prepared by cutting a Pt rod (3.55 mm diameter, 0.125 mm wall thickness) into small 10 mm pieces. These were annealed to remove any stress formed from cutting. One end of each crucible was crimped and sealed with a spot welder. By using the remaining open end, the crucibles were filled with the prepared mixtures. The powdery mixture inside the crucible was pressed, weighed, then dried at 433 ^oC and weighed again. This additional drying step was to remove any moisture that may have been absorbed during this process. The remaining open end of the Pt crucibles were then crimped, sealed and annealed at 433 ^oC.

B.1.2 Experimental Procedure and Analysis

XRD was used to verify the purity of the constituent materials, however, analysis of the As_2O_5 powder found it to be hydrated. After having heated it in the furnace to dehydrated it, moisture was picked up so quickly that even after taking the powder directly to the XRD for analysis right after showed signs of hydration. As such, this warranted the necessity of the additional drying steps to ensure dehydration.

The samples were placed into a small alumina boat and heated to temperatures ranging from 800 to 950 ^oC using a horizontal tube furnace. This was the initial temperature range chosen to examine the two-phase regions and compounds with lower melting points. There were target temperatures as high as 1600 ^oC, however, lower temperatures were chosen first as it was believed that bursting of the capsules would be an issue throughout the entirety of this investigation. The boat was placed by slowly pushing it to the center of the hot zone using a metal wire. Both ends of the tube are sealed with rubber stoppers with one end having a small opening to allow a thermocouple to tightly fit through so the heating zone may be measured. When the heating period was over, the alumina boat was pulled out of the tube by using a metal wire as a hook and having it drop into a metal bowl resting below the open end of the tube.

B.2 Results and Discussion

Samples were found to have burst. While the bursting may be attributed to the volatile nature of As_2O_5, it is also possible that the samples were insufficiently dehydrated during sample preparation. To determine this, the sample preparation method was revised to ensure that moisture would not be a problem. To simplify this additional investigation, only a single mixture was of $MgAs_2O_6$ was used. Capsules were prepared once again, however, they were dried in between every step and the use of a desiccator was introduced. The revised procedure was the following: filling the crucible with the mixture, placing the open crucible in the oven to dry it, weighing it to observe if the mass changes due to dehydration or mixture volatilization, drying, pressing the loose powder, drying, weighing again, drying, cooling in a vacuum-pumped desiccator, crimping the open crucible end closed, drying, cooling in a vacuum-pumped desiccator, spot welding the crimped end to seal it and then annealing the sample. The crucibles were cooled inside a desiccator as they are too hot to handle upon removing from the oven. The desiccators were vacuum pumped

to remove any moisture in the air while cooling. The samples were quenched after annealing to verify that there were no holes in the welds.

Four samples were prepared using the revised methodology and were subsequently heated: one at 850 ^{o}C and three at 950 ^{o}C. Unfortunately, when heating at 950 ^{o}C, as the alumina boat was being pulled out of the furnace, one of the samples had fallen out, but it was recovered and still quenched. The remaining two samples (in addition to the 850 ^{o}C sample) were quenched without problem. The three samples that were quenched without issue were found to not have burst. The dropped sample was found to have burst. In this case, the sample was likely to have burst due to physical trauma. With these results in mind, it was believed that the bursting was moisture related.

The samples were taken to the XRD to be analyzed, including the sample that had burst. One of the samples that was successfully heated to 950 ^{o}C was set aside for EPMA analysis; however, this was ultimately not conducted. To prepare the samples for XRD analysis, the capsules were once submerged under cyclohexane before opening. This was done as a precautionary step to avoid moisture in the atmosphere being absorbed into the samples. While remaining submerged, the capsules were cut opened and emptied. The samples were observed as a white powder. The samples were analyzed while still slightly damp with cyclohexane. XRD results of the successful samples had shown very good agreement with $Mg_2As_2O_7$ and the failed one also displayed peaks matching those of $Mg_3As_2O_8$. This is likely due to As_2O_5 volatizing out the hole of the burst crucible leading to the formation of the less arsenic containing compound. The successful 950 ^{o}C sample had perfect agreement with the XRD database. Not observed, however, was any indication of a glass phase, which was to be expected, as it was previously mentioned based on the optimized phase diagram of MgO – As_2O_5 (Figure 6.1). This would be seen as a bump in the base of the XRD curve in the low angle regions. Seen instead, however, is a relatively flat base. The cause of this is not precisely known. While it may be the result of the glass phase being accidentally being destroyed when cutting and removing the sample from the crucible, the complete absence of a liquid phase in the results is unusual. Attempts were made to reproduce the results, however, recreating the samples proved to be challenging as they were continually bursting when. This highlights the difficulty and care required for sample preparation or it may indicate the need for an even more careful procedure. This also demonstrates the challenges of completing the

experiments and, with the presented methodology and materials used, achieving higher temperatures and examining the key experimental points is currently not feasible.

B.3 Future Considerations

While the experiments may not be currently feasible, that does not mean that they are impossible. It is believed that, with the use of alternative materials and/or methodology, the experiments may be complete successfully and following are suggestions for consideration for future experimental studies.

Thicker Capsules

By using Pt tubes with a thicker wall thickness, the crucibles will be able to withstand a greater change in internal vapor pressure and delay bursting to higher temperatures. The exact relationship of how much thicker the wall needs to be for a given temperature (or vice versa) is not known.

Piston Cylinder (High-Pressure) Experiments

The bursting of the capsules is a result of the internal pressure becoming greater than that of the atmospheric pressure, causing the capsule to physically deform until it ruptures. To prevent this, the capsules are instead heated in a high-pressure environment known as the pressure assembly. A piston presses into the assembly, which contains a (pressure) medium, and a hydrostatic force is applied to the sample. Pressures from 0.5 to 6 GPa may be achieved. This experiment may be conducted at various pressures to determine the melting temperature of compounds. The melting temperature will change according to the pressure, however, with the data collected through this, a trend to observe the change in melting temperature with pressure may be determined and may be used to extrapolate the melting temperature of the compound at standard atmospheric conditions [53].